공학석사 학위논문

Reductive treatment of fluoroarenes using zeolite supported Rh-based catalyst

-Elucidating influence of chemical structure on reduction rate and defluorination-

Rh-zeolite 촉매를 이용한 불화 방향족 탄화수소의 환원처리

-화학적 구조가 환원반응상수 및 탈불화에 미치는 영향 규명-

2020년 8월

서울대학교 대학원

건설환경공학부

안 선 영

Reductive treatment of fluoroarenes using zeolite supported Rh-based catalyst

-Elucidating influence of chemical structure on reduction rate and defluorination-

지도교수 최 정 권

이 논문을 석사 학위논문으로 제출함

2020 년 8 월

서울대학교 대학원

건설환경공학부

안 선 영

안선영의 석사 학위논문을 인준함

2020 년 8 월

위 원 장 김 재 영 (인)

부위원장 최 정 권 (인)

위 원 최 용 주 (인)

Abstract

Reductive treatment of fluoroarenes using zeolite supported Rh-based catalyst

- Elucidating influence of chemical structure on reduction rate and defluorination-

Seonyoung An
Civil and Environmental Engineering
The Graduate School
Seoul National University

This study used zeolite supported Rh-based catalyst and hydrogen as a reductant to reduce fluoroarene, which is also a big part of the chemical industry. Rh/zeolite catalyst was applied for the reductive treatment of fluoroarenes with various structures. The experimented fluoroarenes were fluorobenzene, difluorobenzene, (difluoromethyl)benzene, (trifluoromethyl) -benzene, (pentafluoroethyl) benzene, fluorophenol, fluorotoluene, fluorobenzoic acid, and their pseudo-first-order reaction constant and defluorination yield were compared with each other. The reaction rate of fluorobenzene and difluorobenzene decreased in the order of one substituent (fluorobenzene), ortho (1,2-difluorobenzene), meta (1,3-difluorobenzene), and para (1,4-difluorobenzene). It was the same as the results of other papers. However, perfluoroalkyl groups,

such as trifluoromethyl and pentafluoroethyl, did not react or the defluorination yield was lower than 30%, so the application of Rh catalyst had a limitation in the perfluorinated alkyl structure.

Multiple linear regression analysis was performed to elucidate the effect of structural characteristics of each fluoroarenes on their reaction constants and defluorination yield, except for (trifluoromethyl)benzene, 4-trifluoromethylphenol, (pentafluoroethyl)benzene. To perform multiple linear regression analysis, two or more independent variables were required, and variables capable of representing the structural characteristics of each fluoroarene were selected, such as $\sigma_{position}$, bond dissociation energies (BDE), number of fluorine (No.F), and some chemical properties calculated by SPARC chemical calculator. As a result, the electron affinity, $\sigma_{position}$, and No.F had a significant effect on the reaction rate constant ($Log(k_{obs})$), and the electron affinity, $\sigma_{position}$, BDE, boiling point, and No.F was found to have a significant effect on defluorination yield (DeF yield*). The R^2 value of each regression model was 0.795 for $Log(k_{obs})$ and 0.816 for DeF yield*. Thus, the regression model for defluorination yield was better explained than for the reaction rate constant. In other words, the structural and chemical properties of fluoroarene had a greater effect on the final defluorination yield than the reaction rate. It suggested that not only the defluorination reaction but also hydrogenation occurred by Rh/zeolite catalyst, and the structural and chemical properties of fluoroarene can change the ratio of defluorination/hydrogenation reaction.

Since there were expected to be various intermediates that can be produced through hydrogenation reaction, some of the expected intermediates were quantified when 1-difluoromethyl-2-fluorobenzene and 1-difluoromethyl-3-fluorobenzene were experimented as starting materials. Difluoromethylbenzene, fluorotoluene, toluene, and methylcyclohexane were selected as the expected intermediates, and the concentration was quantified according to the reaction time. As a result, in both cases, the concentration ratio of dimethylbenzene and fluorotoluene compared to the initial concentration was measured very low, and the generated time was similar. In other words, both fluorine attached to the benzene and fluorine of dimethyl could be rapidly defluorinated, and it was suspected that unknown intermediates, which undergo only hydrogenation, not defluorination, might be generated. This phenomenon occurred when two functional groups were in the meta position, such as 1,3-difluorobenzene, 1-difluoromethyl-3-fluorobenzene, and 3-fluorophenol, except for 3-fluorotoluene.

Keyword: Fluoroarene, Hydrodefluorination, Rhodium catalyst, Structure-reactivity relationships

Student Number: 2018-26687

Table of Contents

Contents of Table

Contents of Figures

1. Introduction

1.1. Study Background

Poly- and per-fluorocarbons (PFCs) are manufactured and used for various purposes such as fire-fighting applications, medicine, cosmetics, lubricants, etc[1]. With increasing industrial use of the fluorochemicals, great attention has been shown to the concern of their impact on human health and fate in the environment[2]. Their strong C-F bonds particularly make them recalcitrant in the water and wastewater treatment processes. Therefore, there have been many studies to remove C-F bonds from PFCs.

Among them, catalytic hydrodefluorination is a promising way to treat PFCs[1,3-5]. While C-F bonds in few fluoroarenes such as fluorobenzene and its congeners are known to be reduced to C-H bond in the presence of alumina-supported Rh catalyst[4-6]. However, the applicability of Rh-based catalyst for poly- and perfluoroalkyl groups was not explored.

In this study, we focused on fluoro-aromatic compounds called fluoroarenes. Fluoroarene is also a big part of the chemical industry, especially in the pharmaceutical, thus it is more likely to have been released into the environment[2]. And even more, for workers handling fluoroarences, the organic fluorine level of 1.0-71 ppm have been reported in their blood serum[7]. However, little is known of fluoroarenes having various structures such as fluoromethyl or fluoroethyl groups and their effect on the hydrodefluorination

reaction.

Rebekka and her colleagues found that the reaction rate decreases as the number of fluorine increases and the distance between the substituents increase in the case of the FB series when using Rh-based catalysts[8]. In the case of fluoroarene with a fluoromethyl or fluoroethyl group, it has limitations to test the activity of the catalyst in all cases, because there are too many combinations of each substituent and new fluoroarenes are continuously being produced. Therefore, this study was planned with the expectation that the reactivity of newly synthesized fluoroarene can be predicted by knowing how some basic type or position of fluorine substituent affects the compound reactivity.

1.2. Purpose of Research

The objective of this research is to elucidate the effect of basic fluorine substituent on the reactivity of fluoroarenes, thus predicting the reactivity and defluorination yield of the reaction.

1) Investigate the influence of chemical structure on the removal rate and defluorination yield of fluoroarenes using a Rh/zeolite catalyst
2) Determine structure-reactivity relationships of catalytic reduction of fluoroarenes, and quantify the effect of each substituent.

1.3. Research area

In this study, hydrodefluorination of fluoroarenes was carried out using a zeolite-supported Rh catalyst and H_2 as a reductant under mild aqueous conditions.

1) Various fluorine substituents (fluorine, difluoromethyl, trifluoromethyl, pentafluoroethyl), functional groups (hydroxyl, methyl, carboxylic acid) and their position (one substituent, ortho, meta, para) were dealt with.
2) The pseudo-first-order reaction constant, defluorination yield, and defluorination ratio were calculated to show the reactivity of each fluoroarenes.
3) The relationship between structural properties and reactivity of each fluoroarenes was quantified through multiple regression analysis.

2. Literature review

2.1. Fluoroarene

Fluoroarene means any fluoro-derivative of arene, for example, fluorobenzene, hexafluorobenzene, fluorophenol, and is also called fluoroaromatic. Fluoroarene is used for many purposes such as pharmaceuticals, plant protection agents (herbicides, fungicides), surfactants, refrigerants, intermediates in organic synthesis, and solvents[2]. Even in 1992, it was estimated that businesses involving the sale of compounds containing carbon-fluorine bonds were worth about $ 50 billion per year, and have been growing ever since[9]. Moreover, a SciFinder Search revealed that fluoroarenes are the largest group of commercially available halogenated arenes; the number of registered compounds is as follows; Ar-F (6,336,383), Ar-Cl (6,186,473), Ar-Br (3,407,354), and Ar-I (433,556)[10]. Thus, not surprisingly, significant research efforts have been directed toward C-F cleavage protocols to develop synthetic strategies and so the amount discharged to the environment increased. The compounds gradually accumulate in the environment, reaching concentrations that are hazardous to living organisms[2].

These fluoroarenes are not easily decomposed in the environment. Compared to the relatively activated C-X bonds of halogenated arenes and their equivalents (Ar-X; X=Cl, Br, I), which easily undergo oxidative addition in metal-catalyzed coupling

reactions, the cleavage of C–F bonds in fluoroarenes (Ar–F) is in general significantly more challenging due to their high dissociation energy; they are arguably the strongest bonds that carbon can form (Figure 2.4). They also have a very slow microbial decomposition rate. There have been several studies on the degradation of fluorobenzene and fluorobenzoic acid by bacteria, showing that it takes about 10~45 hours for maximum removal of initial fluoroarene[11–13]. It means that they are strongly resistant to biological degradation and that is why catalytic treatment for the fast decomposition of fluoroarenes has recently been prominent.

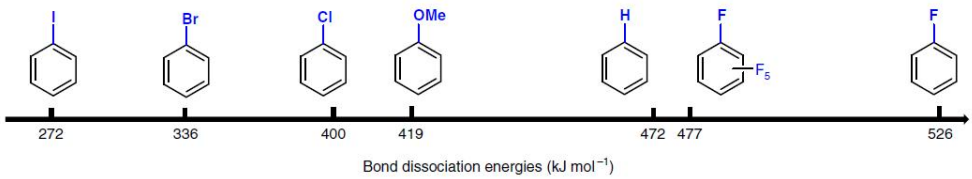

Figure 2.1 Bond dissociation energies (BDE) of halogenated benzenes[10]

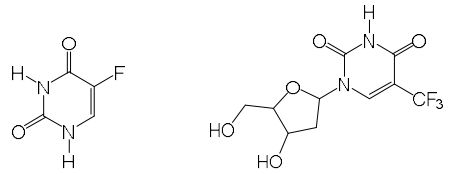

5–Fluorouracil
(anti–cancer)

Trifluridine®
(anti–viral)

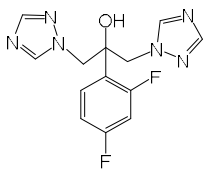

Fluconazole®
(anti–fungal)

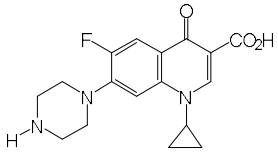

Ciprofloxacin®
(antibacterial)

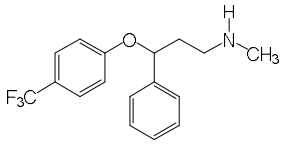

Prozac®
(anti–depressant)

Figure 2.2 Examples of fluorinated pharmaceuticals

2.2. Rhodium catalyst

Rhodium is a highly reactive catalyst on hydrogenation and well known as one of the elements on the three-way catalytic converter for the automobile exhaust gas purification systems. Rhodium catalyst is generally used for hydrogenation and its ability to activate C-F bonds has been attracting attention as a treatment of PFCs has been in the spotlight.

The common oxidation state of rhodium is 3+, but oxidation states from 0 to +6 also exist and hydrodefluorination reaction requires zero-valent Rh(0) which can reduce fluoroarenes. Therefore, to utilize the rhodium catalyst for reduction reaction, the Rh(Ⅲ) should be activated to zero-valent Rh(0), meaning a reduction of rhodium. There are several ways to activate rhodium, such as contacting the $NaBH_4$ solution or flowing hydrogen gas at high temperatures. In this study, hydrogen gas was used for activation of the rhodium when synthesizing zeolite-based rhodium catalysts. The detailed method was described in the method part.

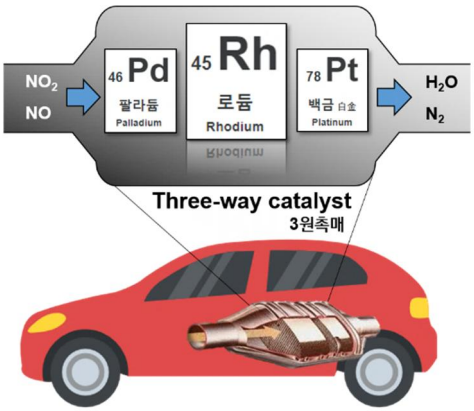

Figure 2.3 Rhodium usage for three-way catalyst in the automobile system

Table 2.1 Oxidation states of rhodium[14]

+0	$Rh_4(CO)_{12}$
+1	$RhCl(PH_3)_2$
+2	$Rh_2(O_2CCH_3)_4$
+3	$RhCl_3$, Rh_2O_3
+4	RhF_4, RhO_2
+5	RhF_5, Sr_3LiRhO_6
+6	RhF_6

2.3. Hydrodefluorination

The most simple C-F bond transformation is hydrodefluorination (HDF) which, shows a surprising mechanistic diversity[9-11]. The reaction formally involves the activation of a carbon-fluorine bond resulted from the introduction of hydrogen to form the hydrogenated products.

The first example of a catalytic HDF reaction was reported by Swarts in 1920, who developed Pt and Ni alloys for the HDF of mono fluorinated arenes using hydrogen gas. However, this method suffers from the inconveniences derived from the need for high temperatures and pressures. Subsequent researchers showed that various transition-metal-mediated catalyst easily cleaves a C-F bond of fluoroarene, such as hexafluorobenzene (C_6H_6), in mild condition[3,5,8,18]. When using a Rh/Al_2O_3-based heterogeneous

catalyst under mild condition (room temperature, 1 atm H_2), the observed fluorinated intermediates indicate that adjacent fluorine substituents are removed preferentially[8].

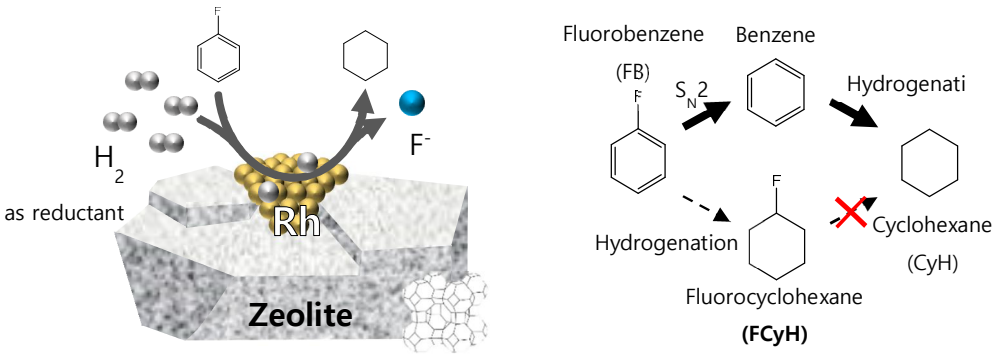

Figure 2.4 Reactions of fluorobenzene with H_2 catalyzed by rhodium catalyst[5]

2.4. Structure–reactivity relationships

For many environmental matrices, experimental constants or coefficients required to assess quantitatively the behavior of a given compound are often not available and, therefore, have to be estimated. In these approaches, one tries to express the free energy of a given in the system of interest by one or several other known free energy terms in a way that they are linearly related. Such approaches are called linear free energy relationships (LFERs). They are useful for predictive purposes and also helpful for checking reported experimental data for consistency[19].

For example, Hammett(1940) found that for substituted benzoic acid the effect of substituents in either the meta or para position on

the standard free energy change of the carboxyl group's dissociation could be expressed as the sum of the free energy change of the dissociation of the unsubstituted compound and the combination of various substituents[19]. As shown in Figure 2.3, plotting $pK_{aH}-pK_a$ values for *meta*- and *para*-substituted phenylacetic acids versus $\sum\sigma_j$ values results in a straight line with a slope, ρ, which is a measure of how sensitive the dissociation reaction is to substitution as compared with substituted benzoic acid. $\sum\sigma_j$ represents the sum of the inductive effect of the compounds.

The Hammett equation, however, does not appear to have been successfully applied to hydrodefluorination reactions of fluoroarenes in aqueous solution. One difficulty in using it relates to the question of an appropriate reference compound. Unsubstituted compounds are generally selected as reference compounds, but non-fluorinated compounds do not undergo defluorination. Correlation can be performed without normalizing reactivity to some reference compound; a further complication, however, is that some substrates undergo base-prompted reaction, whereas reaction rates of other compounds are independent of pH[20]. Therefore, in this study, solution pH 7 was kept in the kinetic experiment to exclude the base-prompted reaction, and multiple linear regression analysis was conducted using non-normalized reactivity and chemical properties of the target materials.

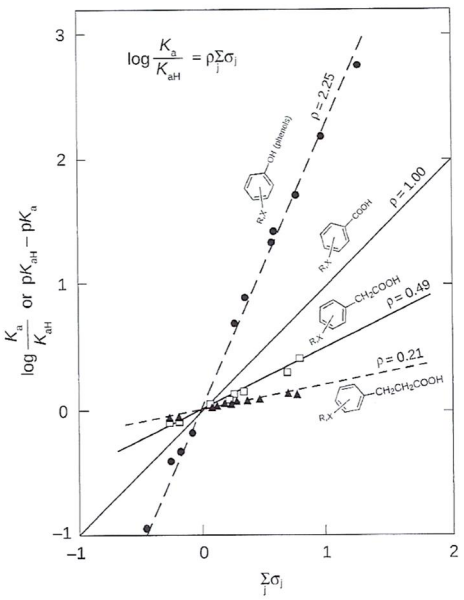

Figure 2.5 Hammett plot for meta- and para-substituted phenols, phenylacetic acids, and 3-phenylpropionic acids; data from Serjeant and Dempsey (1979)[19].

Table 2.2 Hammett constant for some common substituents; data from Dean (1985) and Shorter (1994 and 1997)[19].

Substituent j	σ_{jmeta}	σ_{jpara}	Substituent j	σ_{jmeta}	σ_{jpara}	σ^{-}_{jpara}
– H	0.00	0.00	– OH	0.10	–0.36	
– CH_3	–0.06	–0.16	– OCH_3	0.11	–0.24	–0.12
– CH_2CH_3	–0.06	–0.15	– $OCOCH_3$	0.36	0.31	
– $CH_2CH_2CH_2CH_2$	–0.07	–0.16	– CHO	0.36	0.22	1.03
– $C(CH_3)_3$	–0.10	–0.20	– $COCH_3$	0.38	0.50	0.82
– $CH=CH_2$	0.08	–0.08	– $COOCH_3$	0.33	0.45	0.66
– C_6H_5 (phenyl)	0.06	0.01	– CN	0.62	0.67	0.89
– CH_2OH	0.07	0.08	– NH_2	–0.16	–0.66	
-– CH_2Cl	0.12	0.18	– $NHCH_3$	–0.25	–0.84	
– CCl_3	0.40	0.46	– $N(CH_3)_2$	–0.15	–0.83	
– CF_3	0.44	0.57	– NO_2	0.73	0.78	1.25
– F	0.34	0.05	– SH	0.25	0.15	
– Cl	0.37	0.22	– SCH_3	0.13	0.01	
– Br	0.40	0.23	– $SOCH_3$	0.50	0.49	
– I	0.35	0.18	– SO_2CH	0.68	0.72	
			– SO_3^-	0.05	0.09	

Furthermore, among various variables that can represent the chemical structure, bond dissociation energies (BDE) have been used to describe various chemical transformations as variables to interpret bond strength. The definition of BDE is as follows; BDE for a bond R−F that is broken through the reaction

$$RF \rightarrow R\bullet + \bullet F$$

is defined as the standard−state enthalpy change for the reaction at a specified temperature, here at 298 K.

$$BDE = \Delta Hf_{298} = \Delta Hf_{298}(R\bullet) + \Delta Hf_{298}(\bullet F) - \Delta Hf_{298}(RF)$$

Using these ideas, it is possible to determine the energetics of a wide range of simple but important reactions involving the exchange of a single bond[21]. In this study, BDE of C−F bonds in fluoroarene were calculated based on density functional theory (DFT) for using them as structural variables.

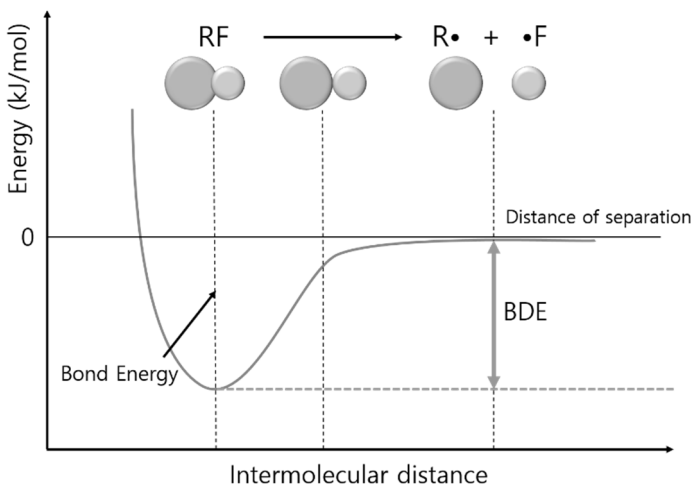

Figure 2.6 Definition of bond dissociation energies (BDE)

2.5. Multiple linear regression analysis

Regression analysis is a statistical technique for estimating the relationship among variables that have reason and result relations. Regression models with one dependent variable and more than one independent variable are called multiple linear regression[22]. In this study, data for multiple linear regression analysis was prepared from the kinetic experiments and computational calculations, which were described in the method part.

Multiple linear regression analysis models are formulated as in the following;

$$y = \beta_0 + \beta_1 x_1 + \beta_2 x_2 + \cdots + \beta_n + \varepsilon$$

y = dependent variable

x_i = independent variable

β_i = parameter

ε = error

The assumption of multiple linear regression analysis is normal distribution, linearity, freedom from extreme values, and having no multiple ties between independent variables.

3. Materials and methods

3.1. Reagents

Hydrogen (99.999%) and nitrogen (99.999%) gas were purchased from Daehan Gas Company (Republic of Korea). Fluorobenzene, (difluoromethyl) benzene, 1,4-difluorobenzene, benzene, 4-trifluoromethylphenol, (trifluoromethyl)benzene, methanol (for HPLC, ≥ 99.9%), dichloromethane, sodium carbonate, sodium bicarbonate, and rhodium(Ⅲ) nitrate hydrate were purchased from Sigma-Aldrich. 1,2-Difluorobenzene, 1,3-difluorobenzene, 1,4-difluorobenzene, 1-difluoromethyl-2-fluorobenzene, 1-difluoromethyl-3-fluorobenzene, 1,4-bis(difluoromethyl)Benzene, 2-fluorophenol, 3-fluorophenol , 4-fluorophenol, 2-fluorotoluene, 3-fluorotoluene, 4-fluorotoluene, 4-fluorobenzoic acid, methylcyclohexane, hexanes (mixed isomers, 60+% n-hexane), and ethyl acetate were purchased from Alfa Aesar. Fluorocyclohexane was purchased from Acros-Organics. Potassium phosphate monobasic, potassium phosphate dibasic anhydrous were purchased Daejung Chemicals & Materials Company.

3.2. Catalyst

The catalyst was prepared with supports zeolite 3A (Wako Pure Chem. Ind. Ltd) as a sieve of 0.34−0.75 μm of particles. Incipient impregnation wetness method was used and the desired rhodium loading was 4 wt%. Rhodium nitrate solution containing an appropriate amount of rhodium was added dropwise to zeolite 3A, mixed and dried overnight in the oven (60 ℃). After completely dried, the powder was thermos−treated to reduce Rh(Ⅲ) to zero−valent Rh(0) by flowing hydrogen gas at high temperature using a tube furnace. Temperature profile for the tube furnace is:

1) Nitrogen: 25 ℃ (room temperature), ramp 20min to 120 ℃, hold 30 min, cooling 30 min
2) Hydrogen: 25 ℃ (room temperature), ramp 40 min to 200 ℃, hold 20 min, ramp 20 min to 400 ℃, hold 120 min, cooling 60 min

The catalyst was stored in a sealed container with silica gel, and no special precautions were taken to avoid exposure to air prior to the batch experiments. The Rh loading rate of 4.1 wt% was measured by the acid extraction method with ICP−OES. Rhodium distributions in the catalyst were examined by field emission transmission electron microscope (FE−TEM, JEM−F200) with a 200 kV acceleration voltage. X−ray photoelectron spectroscopy (XPS) was used to confirm that the rhodium charge state was simultaneously present in trivalent and zero−valent and stable at room temperature. TEM, SEM images, XPS spectra were shown in the Appendix.

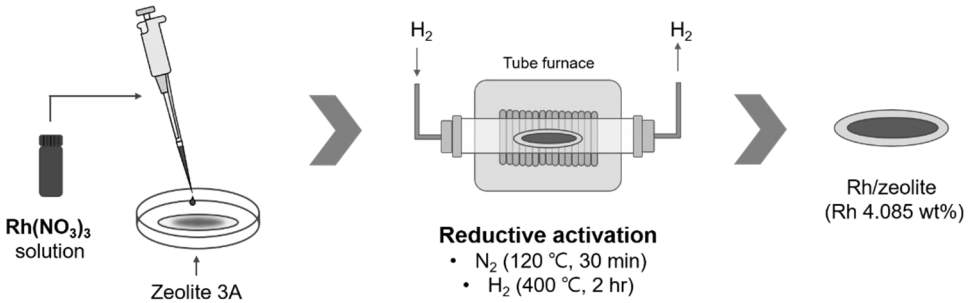

Figure 3.1 Synthesis of Rh/zeolite catalyst and reductive activation method

Table 3.1 Chemical structure of the fluoroarenes used in this study and their abbreviations

Structure	Name/Abbreviations	Structure	Name/Abbreviations
	Fluorobenzene FB		3-Fluorophenol 3FP
	1,2-Difluorobenzene 1,2DFB		4-Fluorophenol 4FP
	1,3-Difluorobenzene 1,3DFB		2-Fluorotoluene 2FT
	1,4-Difluorobenzene 1,4DFB		3-Fluorotoluene 3FT
	(Difluoromethyl)benzene DFMB		4-Fluorotoluene 4FT
	1-Difluoromethyl-2-fluorobenzene DFM-2FB		4-Fluorobenzoic acid 4FBA
	1-Difluoromethyl-3-fluorobenzene DFM-3FB		(Trifluoromethyl)benzene TFMB
	1,4-Bis(difluoromethyl)benzene 1,4DFMB		4-(Trifluoromethyl)phenol 4TFMP
	2-Fluorophenol 2FP		(Pentafluoroethyl)benzene PFEB

3.3 Batch experiments

A mixture of phosphate buffer (pH 7, 10 mM, 99 mL), Rh/zeolite catalyst (0.1g/L) in a 120 mL serum bottle was stirred using an electronic magnetic stirrer in a water bath (20±2 ℃) for 30 min to allow the catalyst to disperse well. Buffer was used to preventing the slight increase in pH observed in the un-buffered system and shown to not affect the determined rate constants. The solution was purged with H_2 for 5 min prior to initiation of the reaction and kept under 1 atm during the reaction. Starting fluoroarenes (20 mM, 1 mL, dissolved in methanol) was added to the reactor through the septa using glass syringes. Vigorous stirring was continued during the reaction. Batch experiments were performed triplicate for each target fluoroarene.

Aliquots of 0.5 mL were sampled with a glass syringe and added to 3 mL organic solvent in a 4 mL amber vial. The water sample and the organic solvent separated into two layers were mixed vigorously for 1 min using the vortex mixer and allowed to equilibrate for 15-19 hours (overnight) for partitioning into the organic solvent. Due to the efficiency of the extraction, water samples did not require filtration. The organic solvent used for extraction was different depending on the partitioning coefficient of each fluoroarenes, as shown in Table 3.2.

For every control samples, fluoride was not detected, which means there was no reaction by hydrogen without the catalyst.

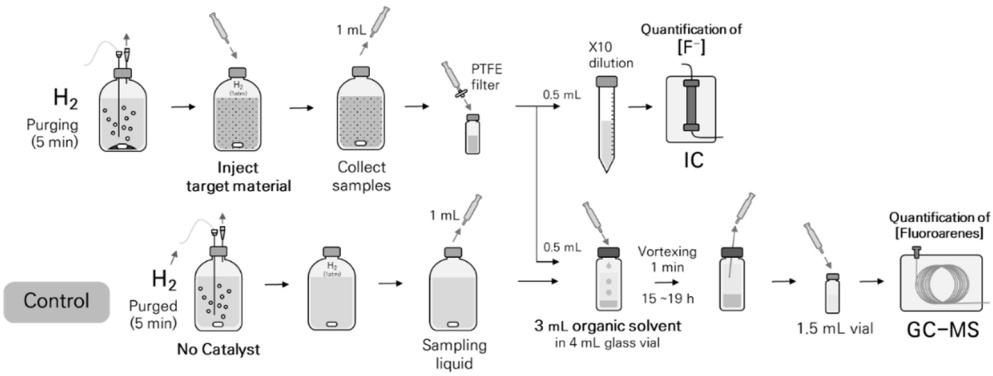

Figure 3.2 Scheme of the kinetic experiment

Table 3.2 Organic solvent for extraction of each fluoroarene

Organic solvent	Hexanes		Dichloromethane	Ethyl acetate	
Fluoroarenes	FB	DFMB	2FP	TFMB	2FT
	1,2DFB	DFM-2FB	3FP	1,4TFMB	3FT
	1,3DFB	DFM-3FB	4FP	PFEB	4FT
	1,4DFB	1,4DFMB		4TFMP	

*4FBA was measured by LC-MS without extraction procedure

3.4 Analytical methods

Benzene, toluene, methylcyclohexane, all fluoroarenes extracted by organic solvents, except fluorobenzoic acid, were analyzed by an Agilent 7890B gas chromatograph (GC) linked to an Agilent 5977B Mass Selective Detector (MSD). The column used was an HP-5MS 5% phenyl methyl silox (30 m × 250 μm × 0.25 μm). Temperature profiles applied were different for fluoroarenes as shown in Table 3.3. Calibration standards were prepared using the same solvent with the extraction solvent for each material. The oven temperature was shortened according to the retention time of the target material.

Agilent 1260 series LC system (Agilent, Waldronn, Germany) coupled with an Agilent 6120 single-quadrupole mass analyzer was used for the analysis of 4-fluorobenzoic acid. The chromatographic runs were carried out on a single Zorbax Extend C18 (2.1 × 150 mm, 1.8 μm) column from Agilent Technologies. Mixtures of acetonitrile (solvent A) and 0.1% formic acid in water (solvent B) were used as the mobile phase eluents. The eluent gradient time profile was as follows: 90% A at t = 0 min, decreased to 20% A from 0 min to 3 min, held at 20% A for 2 min, increased to 90% A from 5 min to 6 min, and re-equilibrated from 6 min to 20 min. The injection volume was 5 μL and the column temperature was set at 40 ℃. The elution flow rate was maintained at 0.2 mL/min. Electrospray ionization MS in the negative mode was used for 4-fluorobenzoic acid. The following MS settings were used: drying gas (i.e., N2) flow rate of 7.0 L/min, nebulizer pressure of 50 psi, drying gas temperature of 350 °C, capillary voltage of 1500 V (positive) and 4500 V (negative), and fragmentor voltages of 100 V.

Ion chromatography (ICS-1100, Thermo Scientific) was used for the analysis of the concentration of fluoride in the bulk samples. The sample was separated on Dionex IonPac AS23 (250 mm × 4.0 mm) column with 4.5 mM Na_2CO_3/$NaHCO_3$ as eluent at a flow rate of 1 mL/min and detected by the suppressed conductivity detector. The detection limits of fluoride were 0.05 mg/L.

Table 3.3 GC Oven temperature profiles applied for fluoroarenes and other arenes

	Temperature profiles	Materials
Method 1	35 ℃ (2 min), ramp (6 ℃/min) to 70 ℃ (3 min)	FB, 1,2DFB, 1,3DFB, 1,4DFB, DFMB, DFM-2FB, DFM-3FB, 1,4DFMB, 2FT, 3FT, 4FT, TFMB, 4TFMP, PFEB, and their intermediates
Method 2	100 ℃ (2 min), ramp (6 ℃/min) to 125 ℃ (3 min)	2FP, 3FP, 4FP, and their intermediates

3.5. Calculation methods

Bond dissociation energies (BDE) were calculated for each fluoroarenes by GAMESS software. The calculation method was M06-2X hybrid functional with an SMD solvation model to consider the polar properties of water molecules around. Geometry optimization with 6-31+G* basis set and single point energy and Hessian calculation with 6-311++G** were performed. All values were given at 298 K by classifying the fluorine directly bound to benzene and fluorine of the difluoromethyl group. The BDE calculation formulas were as below.

$$H^0\ (298K) = E_0 + ZPE + H_{trans} + H_{rot} + H_{vib} + RT$$

$$BDE\ (298K) = H^0\ (R\bullet) + H^0(\bullet F) - H^0\ (RF)$$

ZPE : Zero-point energy, which is the lowest possible energy that a quantum mechanical system may have

Online SPARC chemical calculator was used to obtain physical and chemical properties of fluoroarenes. SPARC uses computational algorithms based on fundamental chemical structure theory to estimate a variety of reactivity parameters. The references were noticed on ARChem (Automated Reasoning in Chemistry). Multiple linear regression analysis for each dependent variables Log(k_{obs}) and DeF yield* was performed by SPSS software.

4. Results and discussions

4.1. Reaction kinetics and defluorination yield

It should be noticed that not only defluorination but also hydrogenation are considered in the removal of target fluoroarenes. In other words, the defluorination reaction needs to be distinguished from the hydrogenation reaction. As conducting the reaction with Rh/zeolite catalyst on targeted fluoroarenes, fluoride was not always generated as much as the proportion of target removed. This result shows that the Rh/zeolite catalyst can reduce not only C−F bonds but also double bonds of benzene rings, so that makes benzene structure to saturated structure like cyclohexane.

4.1.1. Pseudo−first−order reaction constant

Pseudo−first−order kinetics were observed for the degradation of the fluoroarenes. Hydrogen was assumed to be constant and available in excess during the reaction. Pseudo−first−order rate constants (k_{obs}) were obtained by linear regression. Most of the fluoroarenes are removed by more than 90% within an hour, except 1,4DFB, 3FP. Compared with the result of Rebekka (2012), it was confirmed that the Rh−normalized rate constant of FB was much higher but that of 1,3DFB and 1,4DFB was lower than Rebekka' s results. These results show that even with the same rhodium catalyst, the activity

of the catalyst may vary depending on the type of support.

Table 4.1 Comparison of the pseudo-first-order rate constant of different paper results considering the experimental conditions

Varialbe	Unit	Rh/zeolite			Rh/alumina[1)]		
		FB	1,3DFB	1,4DFB	FB	1,3DFB	1,4DFB
k_{obs}	min^{-1}	0.6026	0.0226	0.0136	0.0617	0.0317	0.0367
k_{obs-Rh}	$min^{-1}(mg_{Rh}/L)^{-1}$	0.1470	0.0055	0.0033	0.0326	0.0168	0.0194
C_0[3)]	μM	200			100		
C_{Rh}[4)]	mg_{Rh}/L	4.1			1.89		
Volume	mL	100			164		

1) Rebekka (2012)

2) $k_{obs-Rh} = k_{obs} / C_{Rh}$

3) C_0 : Initial concentration of the fluoroarene

4) C_{Rh} : Concentration of rhodium in the solution

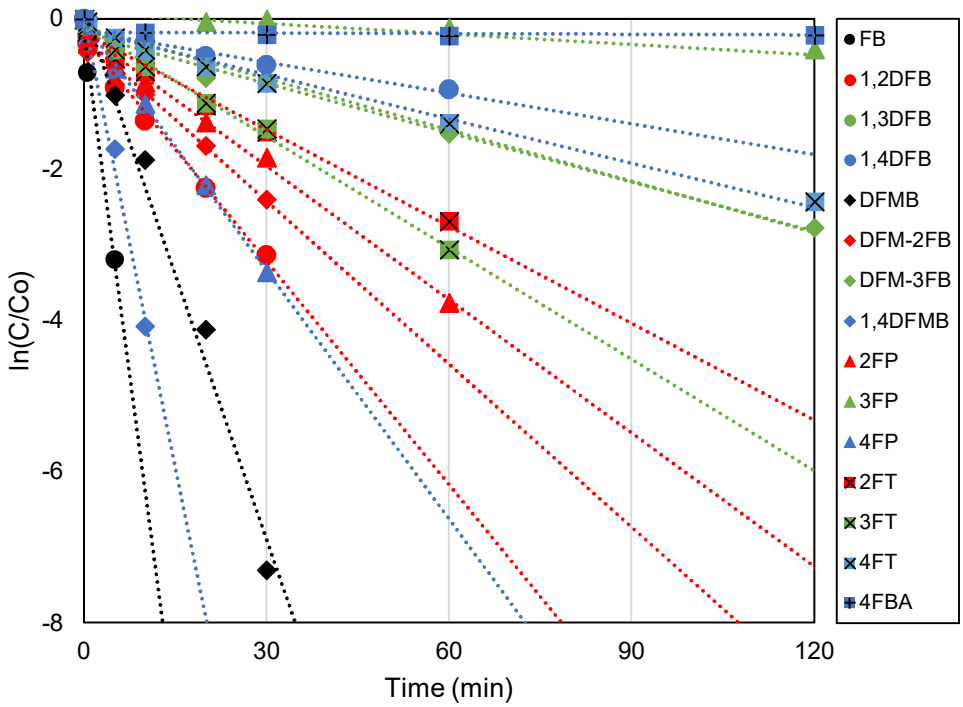

Figure 4.1 Pseudo-first-order kinetic plot of fluoroarene removal by Rh/zeolite catalyst (blank: one substituent, red: ortho, green: meta, blue: para)

4.1.2. Defluorination yield

There is a need to confirm not only how fast the reaction occurs, but also how much defluorination occurs in the overall reaction mechanism. Thus, the fluoride concentration over time during the reaction was measured, and the values were expressed as DeF Yield and DeF ratio as the following definition.

$$\text{DeF yield} = [F^-]_t/[FA]_o$$

$$\text{DeF yield}^* = [F^-]_t/[FA]_o/(\text{No.F})$$

$$\text{DeF ratio}^* = [F^-]_t/([FA]_o-[FA]_t)/(\text{No.F})$$

$[F^-]_t$: Concentration of fluoride at time t [μM]

$[FA]_t$: Concentration of fluoroarene at time t [μM]

$[FA]_o$: Initial concentration of fluoroarene [μM]

No.F : Number of fluorine per molecule

DeF yield is the ratio of the fluoride concentration to the initial concentration of the target material. DeF ratio is the ratio of the concentration of fluoride to the amount of removed target material, meaning that the defluorination mechanism is dominant when the closer the DeF ratio is to 1. The superscript star (*) means normalization by the number of fluorine in the target molecule. All concentration ratio was based on molar concentration.

Defluorination occurred in fluoro and difluoromethyl group, but

much less or no in the trifluoromethyl group. In the case of 4TFMP, it was confirmed that defluorination could occur in the trifluoromethyl group when the hydroxyl group existed in the molecule, but the DeF yield was low to less than 20%. The initial concentration was maintained in the control test when minimizing the headspace volume to prevent it from being volatilized. In other words, the main mechanism of removal of 4TFMP was not defluorination but hydrogenation. Likewise, the main removal mechanism of TFMB and PFEB was expected to be hydrogenation.

Table 4.2 Pseudo-first-order reaction constants and DeF yields of the reaction in the presence of Rh/zeolite catalyst

Fluoroarene	k_{obs}	$Log(k_{obs})$	DeF yield	DeF yield*
	[min^{-1}]		[mol/mol]	[mol^{-1}]
FB	0.6026	−0.220	0.947	0.947
1,2FB	0.0982	−1.008	1.700	0.850
1,3FB	0.0226	−1.646	1.459	0.729
1,4FB	0.0136	−1.866	1.281	0.641
DFMB	0.2338	−0.631	2.005	1.003
DFM-2FB	0.061	−1.180	2.409	0.803
DFM-3FB	0.0211	−1.676	0.884	0.295
1,4DFMB	0.3962	−0.402	3.442	0.861
2FP	0.0589	−1.230	0.633	0.633
3FP	0.0037	−2.432	0.798	0.798
4FP	0.1087	−0.964	0.950	0.950
2FT	0.0468	−1.330	0.997	0.997
3FT	0.0485	−1.314	0.633	0.633
4FT	0.0196	−1.708	0.995	0.995
4FBA	0.0003	−3.523	0.387	0.387
TFMB	0.0069	−4.976	N.D[1)]	−
4TFMP	0.0085	−4.768	0.341	0.114
PFEB	0.0110	−1.959	1.356	0.271

1) N.D: None detected

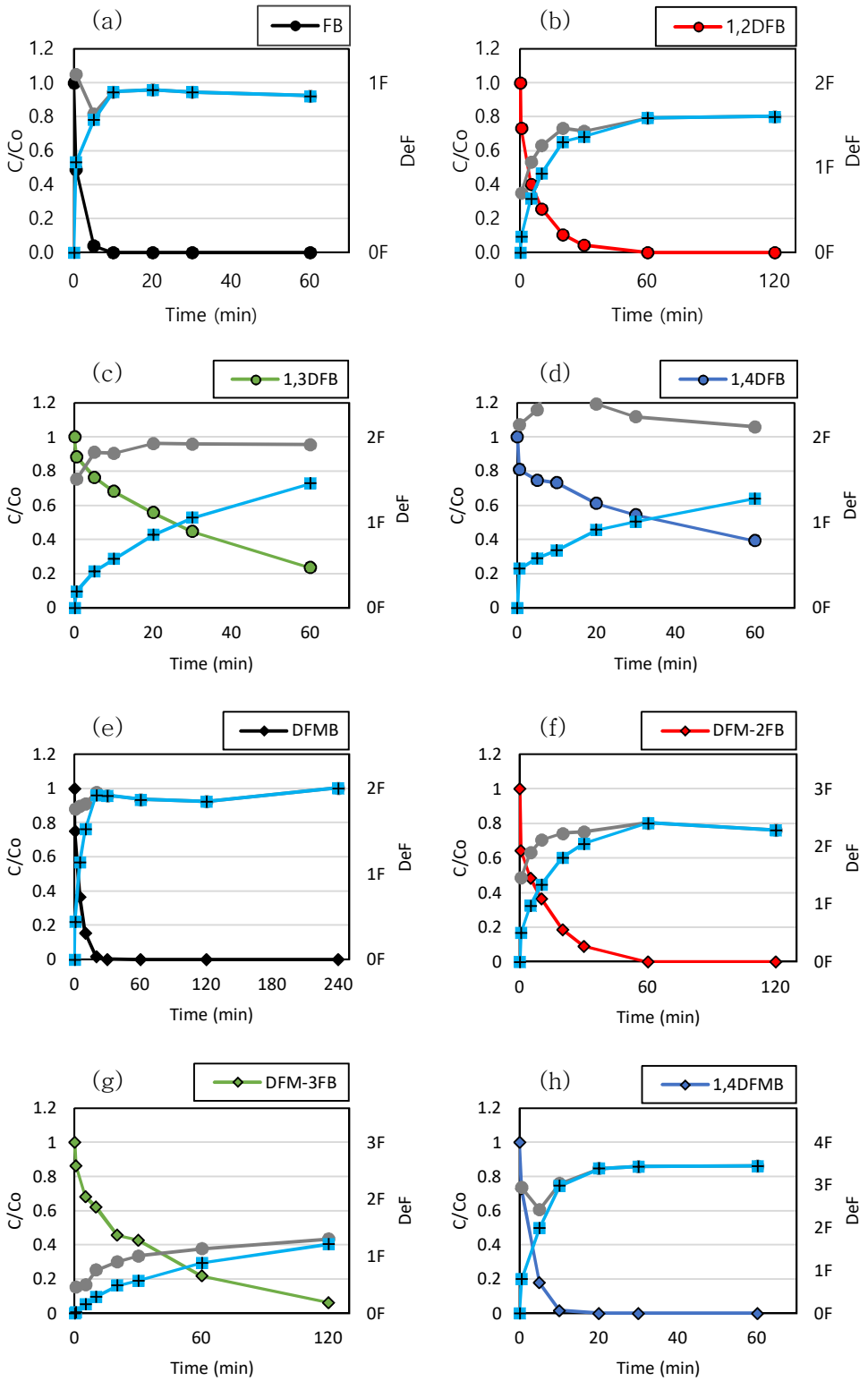
(a)
FB
C/Co
DeF
Time (min)
(b)
1,2DFB
(c)
1,3DFB
(d)
1,4DFB
(e)
DFMB
(f)
DFM-2FB
(g)
DFM-3FB
(h)
1,4DFMB

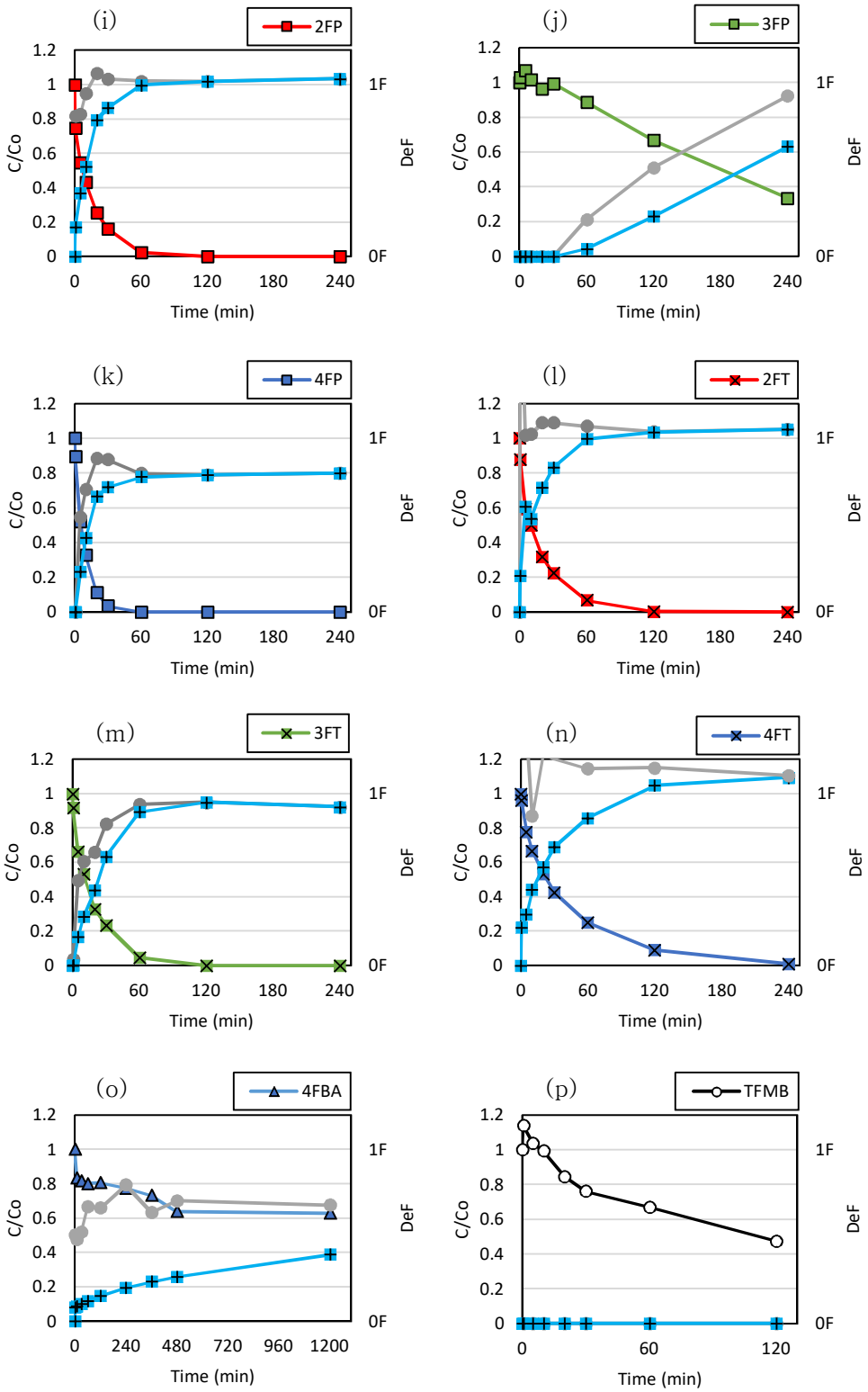
(i)
2FP
(j)
3FP
(k)
4FP
(l)
2FT
(m)
3FT
(n)
4FT
(o)
4FBA
(p)
TFMB
C/Co
DeF
1F
0F
Time (min)
0
60
120
180
240
480
720
960
1200
0.2
0.4
0.6
0.8
1
1.2

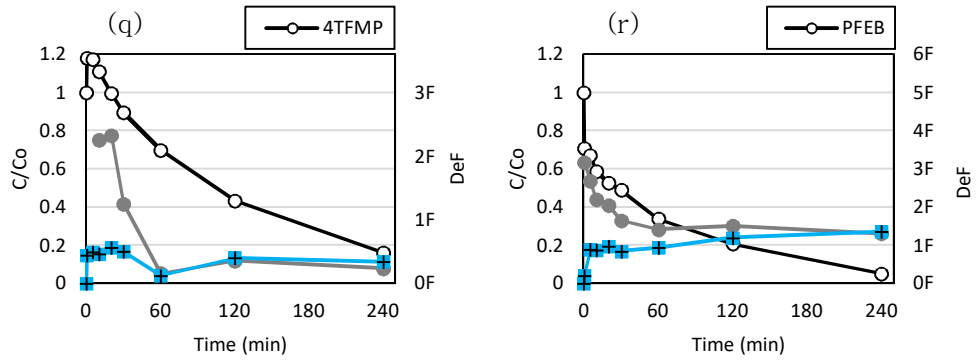

Figure 4.2 Graphs of fluoroarene removal and defluorination yield versus reaction time at pH 7 (phosphate buffer, 10 mM) (✚; DeF yield, ● ; DeF ratio*)

The correlation between Log(k_{obs}) and DeF yield showed weak positive correlations. In other words, rapid removal did not necessarily lead to defluorination. Thus, it was needed to examine the properties of each fluoroarene that affects both Log(k_{obs}) and DeF yield.

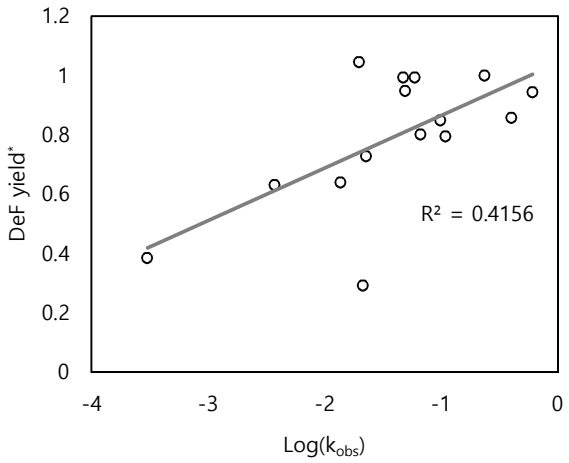

Figure 4.3 Correlation analysis between DeF yield* and Log(k_{obs}) of fluoroarenes

4.2. Effect of structural properties

4.2.1. Effect of the number of fluorine and substituent position

In this study, the reaction rate, and DeF yield* were compared by classifying the number of fluorine (No.F) and the position of the substituent. Fluoroarene with trifluoromethyl or pentafluoroethyl group was excluded from the comparison because the reaction rate was slow compared with other fluoroarenes, the DeF yield was also low or the defluorination reaction did not occur.

In Figure 4.4-(a), No.F did not significantly affect the reaction rate range. On the other hand, in Figure 4.4-(b), it was found that the reaction rate range decreased in the order of one substituent, ortho, and meta position, but the tendency was not continued in the case of para position. Therefore, it was difficult to explain the reactivity of fluoroarene containing difluoromethyl or other functional groups based on only the No.F and position of substituents shown in the existing references. To compensate for this, in the next part, the reactivity was examined according to the type of fluorine substituent and other functional groups.

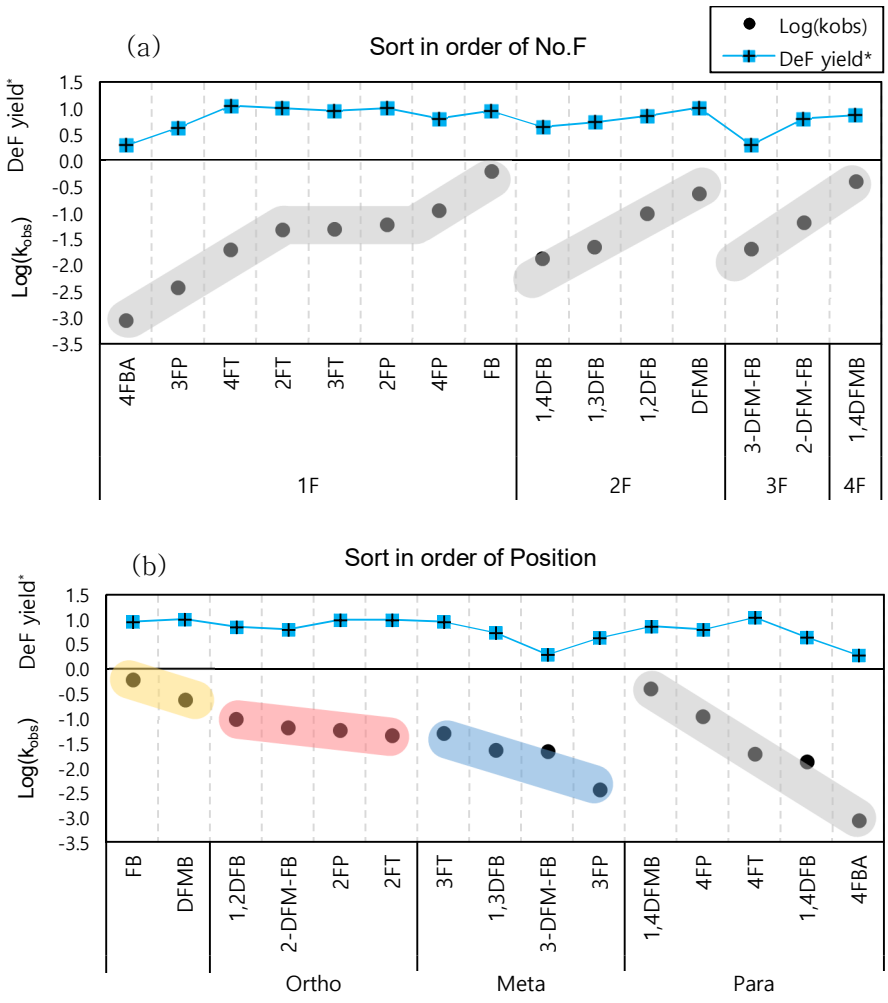

Figure 4.4 Log(k_{obs}) and DeF yield of fluoroarenes in order of (a) number of fluorine (No.F), and (b) position of substituent

4.2.2. Effect of substituent type

There is a difference in DeF yield when comparing fluorine of difluoromethyl substituent group and fluorine directly bound to benzene. In the case of 2DFB and DFM−2FB, the almost maximum amount of fluoride was generated at the target to be removed. In the case of meta−position, the rate constant of DFM−3FB was similar to

3DFB but the final DeF yield* was higher than that of 3DFB, as shown in Figure 4.2 (c) and (g). Different defluorination preferences of the fluorine and difluoromethyl substituents were expected, so DFM-2FB and DFM-3FB were re-experimented to confirm the intermediates. (Difluoromethyl)benzene (DFMB), fluorotoluene (FT), and toluene (T) were selected as the intermediate, and methylcyclohexane (MeCyH) was selected as the final reductant.

As shown in Figure 4.5, the main intermediate of DFM-FB was toluene. DFMB and FT were sharply increased but had a lower proportion compared to the target material and were subsequently removed and also similar in the generated time as well as the C/C_0 ratio. It means that the difference of DeF yield of fluorine bound to benzene and fluorine of difluoromethyl was not due to the substituent type, but the position of the substituent. It was also confirmed that the structural difference had a greater effect on the DeF yield than the reaction rate. The cause was expected because the resonance effect from the π-bond of the arene was higher when it was the ortho than the meta. What was still unknown is the presence of undetected intermediates that did not undergo defluorination but only hydration reaction.

Toluene, the major intermediate in the reduction of DFM-FB, was reduced to MeCyH over time, and MeCyH was expected as a final product in the reduction reaction. However, MeCyH decreased after an hour and the fluoride concentration reached equilibrium, meaning that MeCyH was evaporated from solution to the headspace. The water-based solubility of MeCyH (0.014 g/L at 25℃) is

relatively low than that of toluene (0.52 g/L at 20℃), and it supports the fact that MeCyH had been evaporated. As a result, the reaction pathway of DFM-FB was shown in Figure 4.6.

The reaction rate of fluoroarenes with hydroxyl, methyl, and carboxylic acid group was all lower than that of fluorobenzene, and so did DeF yield*. Fluoroarene with these functional groups did not show a significant difference in the BDE of the C-F bond (Table 4.3) but in the reaction rate and DeF yield* depending on the position of the substituent. Thus, the position of the substituents has a greater effect than the BDE of the C-F bond on the reaction rate or DeF yield, even in the presence of a non-fluorine functional group.

In the presence of the carboxylic acid group, the reaction rate and DeF yield significantly decreased, which appeared to be due to the positive electron affinity of the molecule. High stability of dissolved 4FBA was also expected since 4FBA has a high anion ratio (pKa = 4.14) under experimental conditions of pH 7. Therefore, the Rh/zeolite catalyst seemed to have a limitation in reduction treatment with fluoroarenes that have high positive electron affinity, considering that electron affinity was positive for only 4FBA, while all other comparison fluoroarenes were negative for electron affinity.

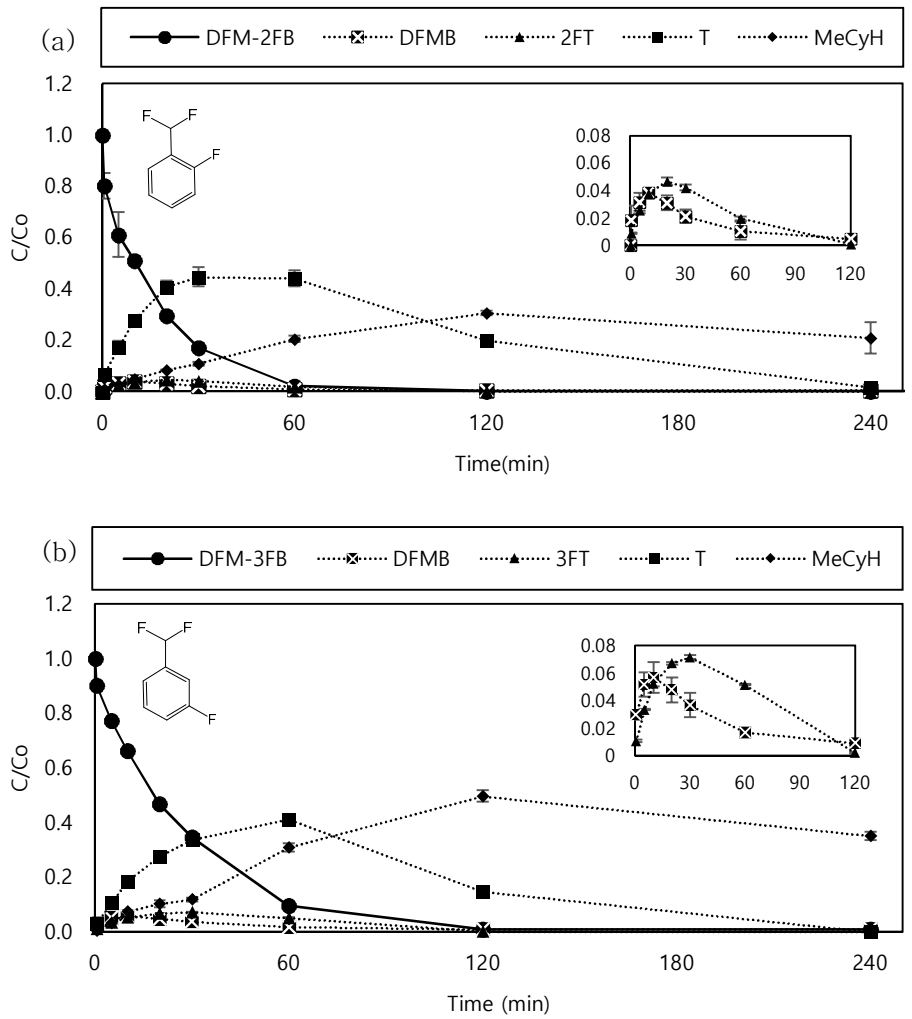

Figure 4.5 Detail of intermediate growth and decay traces during degradation of (a) DFM−2FB and (b) DFM−3FB

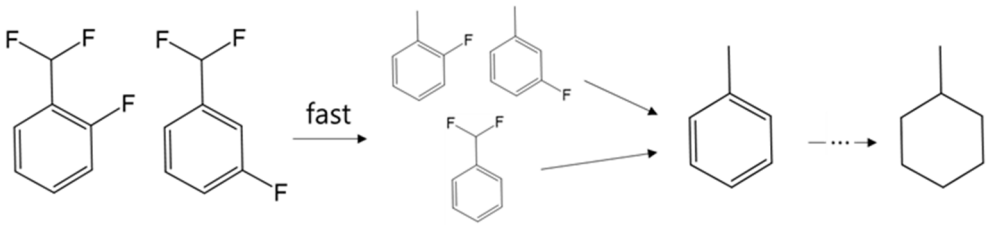

Figure 4.6 Reduction pathway of difluoromethyl−fluorobenzene by Rh/zeolite catalyst

4.3. Structure–reactivity relationships

4.3.1. Selection of variables

According to the previous results, the trend of the reaction rate was not clearly shown depending on the number of fluorine contained in the molecule or the position of the substituents. It means that other variables affected the reactivity of fluoroarenes, thus several chemical properties and new variables suitable for describing fluoroarene were obtained to determine the structure–reactivity relationships using multiple linear regression.

First, the variable representing the position of substituent was needed. Thus, the variable $\sigma_{position}$ was derived, which shows structural properties, based on the fluoro–substituent (FB, 1,2DFB, 1,3DFB, 1,4DFB). The method of deriving the $\sigma_{position}$ is as follows. A linear equation with the slope of −1, and the y–intercept of −0.220 (Log(k_{obs}) of fluorobenzene) was obtained, and then x values were calculated by substituting Log(k_{obs}) of 1,2DFB, 1,3DFB, 1,4DFB for y values. This x values can be understood as the effect of the structural properties on the reaction rate and were defined as $\sigma_{position}$ (one substituent=0.000, ortho=0.788, meta=1.426, para=1.646) (Figure 4.7). The $\sigma_{position}$ was applied to other fluoroarene as shown in Figure 4.8.

Chemical properties of fluoroarenes, such as boiling point (BP), vapor pressure (VP), solubility, electron affinity (EA), and density, were calculated by using SPARC chemical calculator. BP, VP,

solubility, and density were expected to have an indirect effect on catalytic reaction, such as interaction with water molecules or zeolite support. EA was considered to have a correlation with catalytic reaction since it has a high correlation with LUMO energies[23].

The experimental values ($Log(k_{obs})$) as a dependent variable and independent values calculated by SPARC and GAMESS were shown in table 4.3 and Figure A.6.

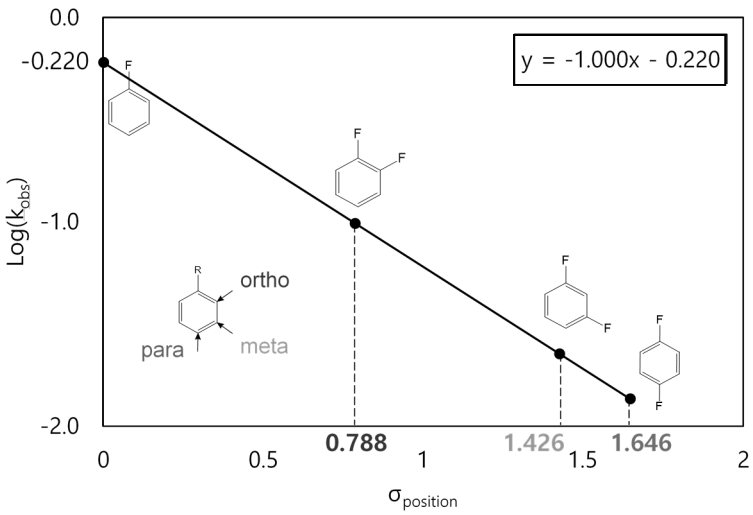

Figure 4.7 The setting of $\sigma_{position}$ variable standardized with fluorobenzenes

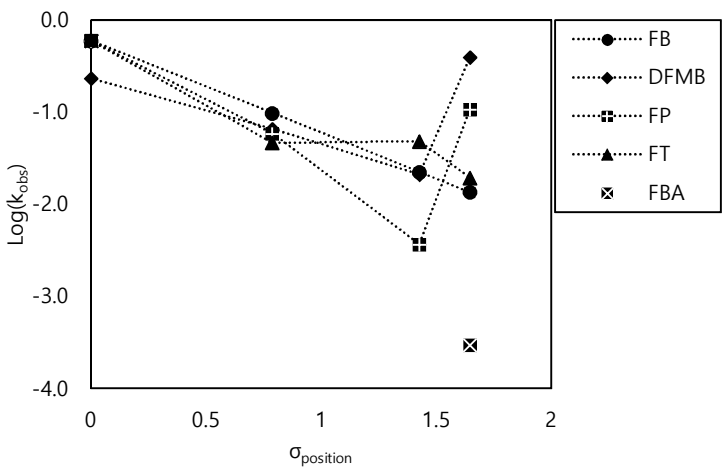

Figure 4.8 $Log(k_{obs})$ values of fluoroarenes versus $\sigma_{position}$ according to substituent type

Table 4.3 Dependent variable (Log(k_{obs})) and independent variables used in multiple linear regression analysis

	Log(k_{obs})	BP[1)]	VP[1)]	Solubility[1)]	EA[1)]	Density[1)]	BDE[2)]	No.F	$\sigma_{position}$
	[−]	[℃]	[Log(atm)]	[Log(mol/L)]	[eV]	[g/cm^2]	[kJ/mol]	[−]	[−]
FB	−0.220	89.29	−0.99	−1.83	−0.81	1.01	529.357	1	0.000
1,2FB	−1.008	98.07	−1.20	−1.98	−0.46	1.16	520.468	2	0.788
1,3FB	−0.646	82.20	−0.91	−2.00	−0.44	1.15	528.064	2	1.426
1,4FB	−1.866	87.88	−1.01	−1.94	−0.43	1.15	527.540	2	1.646
DFMB	−0.631	116.0	−1.64	−2.18	−0.86	1.09	457.934	2	0.000
DFM−2FB	−1.180	119.5	−1.79	−2.21	−0.30	1.22	462.715	3	0.788
DFM−3FB	−1.676	119.1	−1.76	−2.31	−0.29	1.20	454.574	3	1.426
1,4DFMB	−0.402	137.2	−2.38	−2.68	−0.56	1.22	452.439	4	1.646
2FP	−1.230	150.6	−2.47	0.09	−0.65	1.22	513.616	1	0.788
3FP	−2.432	171.1	−2.92	1 (Miscible)	−0.76	1.23	517.934	1	1.426
4FP	−0.964	170.7	−3.00	0.25	−0.78	1.23	516.065	1	1.646
2FT	−1.330	119.0	−1.59	−2.32	−0.62	1.00	518.783	1	0.788
3FT	−1.314	116.5	−1.53	−2.38	−0.62	0.99	517.641	1	1.426
4FT	−1.708	118.5	−1.57	−2.38	−0.62	0.99	516.726	1	1.646
4FBA	−3.523	233.9	−5.45	−2.18	0.43	1.30	517.695	1	1.646

1) Chemical properties that were calculated by using SPARC chemical calculator (Temperature : 25℃, Pressure : 760 torr)

2) BDE: Bond dissociation energy based on water solution (In case of DFMB and TFMB series, the C−F BDE between benzene ring are written first and fluorine and C−F BDE from fluoromethyl group are written later with star mark*.)

4.3.2. Multiple linear regression analysis

Multiple linear regression analysis for each dependent variables Log(k_{obs}) and DeF yield* was performed using all of the independent variables, as shown in Table A.2 and Table A.3. To discriminate the collinearity between variables, variance increase factors (VIFs) were examined and t-test was conducted for each parameter. If VIF equal or higher than 10, there is multicollinearity between variables[22]. When looking at Table A.2 and A.3, most of VIF values were higher than 10. In the t-test results for each variable, the variable corresponding to the Sig. value of less than 0.05 could be interpreted as a significant variable in multiple regression, however, most of variables with the Sig. value of much higher than 0.05 was in Table A.2 and A.3. Thus, by excluding the variables in order of the highest VIF value and the highest Sig. value, it was possible to obtain the results with all VIF less than 10 and Sig. value less than 0.05 when electron affinity, as shown in Table 4.4 and 4.5. In both cases, R^2 was the highest when the entire variables were included and lower R^2 was obtained when more variables were excluded. Finally, two regression models with 0.795 of R^2 for Log(k_{obs}) and 0.816 of R^2 for DeF yield* were obtained.

The greater the magnitude of t-value, the greater the evidence against the null hypothesis. The criterion is that the independent variables have an effect on the dependent variable when the $|t\text{-value}| \geq 1.96$, and can be regarded as a positive effect when it has positive t-value and a negative effect when it has negative t-value.

In the results of the regression analysis, the magnitude of the t-value of electron affinity was the largest as the negative numbers, indicating that the reaction rate and DeF yield* decreased as the electron affinity increased. The larger the electron affinity, the stronger the molecule tends to acquire electrons[24]. In this reaction, fluorine was brought out with electrons from the molecule for defluorination to occur, thus the reaction of losing electrons in the molecule became difficult.

The $\sigma_{position}$ also had a negative effect on both of the dependent variables, meaning that the reaction rate was lower when the substitution position was more distant. This result was the same as the results of polyfluorobenzene's reduction[8]. On the contrary, No.F had a positive effect on the Log(k_{obs}) and DeF yield* when considering various substituents and it was opposite of the results of FB and DFB. In this study, it was because there were more types of fluoroarenes containing only one fluorine atom and their reaction rate constants and DeF yields were often lower than others were. Therefore, No.F could appear differently with a positive or negative effect depending on the range of the target substance.

BDE had a more significant effect on DeF yield* than reaction rate constant. Thus, it was confirmed that the strength of the C-F bond depending on the chemical structure was an appropriate variable for predicting the efficiency of the defluorination ability of Rh/zeolite catalyst to fluoroarenes, not the reaction kinetics. It was peculiar that the t-value of BDE was positive, which seems to be due to the result that BDE of fluorine from difluoromethyl was calculated lower than

that of fluorine bound to benzene and the DFMB series showed lower overall reaction rate constant and DeF yield than the DFB series.

In the case of the boiling point, although it did not seem to correlate with the DeF yield superficially, it was expected that the reaction was indirectly influenced by the fact that the positive t-value was quite large. For example, a high boiling point means that the intermolecular attraction force is large, so these properties might have influenced the coordination between the target substance and the rhodium particle on the catalyst.

Table 4.4 Results of ANOVA test and coefficients from multiple linear regression analysis with Log(k_{obs}) as a dependent variable

Model Summary			
R	R^2	Std. Error of The Estimate	Durbin−Watson
0.892	**0.795**	0.419429	2.525

ANOVA					
	Sum of squares	df	Mean square	F	Sig.
Regression	7.498	3	2.499	14.207	0.000
Residual	1.935	11	0.176		
Total	9.433	14			

Coefficients				
	Coefficients	t	Sig.	VIF
(Constant)	−2.414	−5.438	0.000	
Electron Affinity	−1.712	−4.390	0.001	1.206
$\sigma_{position}$	−0.468	−2.223	0.048	1.188
No.F	0.376	3.186	0.009	1.025

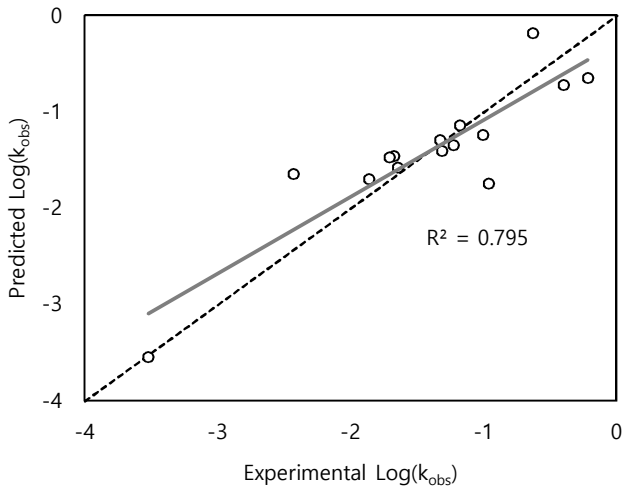

Figure 4.9 Correlation between experimental values and predicted values of Log(k_{obs}) by multiple linear regression

Table 4.5 Correlation between experimental values and predicted values of DeF yield* by multiple linear regression

Model Summary			
R	R^2	Std. Error of The Estimate	Durbin−Watson
0.903	**0.816**	0.121379	1.845

ANOVA					
	Sum of squares	df	Mean square	F	Sig.
Regression	0.586	5	0.117	7.959	0.004
Residual	0.133	9	0.015		
Total	0.719	14			

Coefficients				
	Coefficients	t	Sig.	VIF
(Constant)	−4.825	−2.912	0.017	
Electron Affinity	−0.813	−5.112	0.001	2.394
$\sigma_{position}$	−0.256	−3.470	0.007	1.735
BDE	0.008	3.138	0.012	5.951
Boiling point	0.006	3.795	0.004	3.789
No.F	0.270	2.948	0.016	7.385

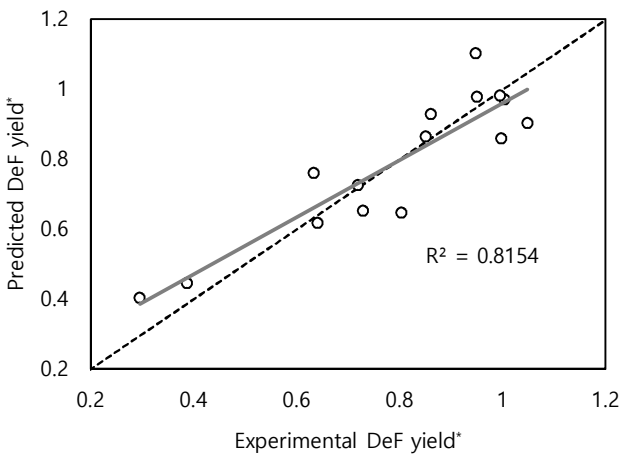

Figure 4.10 Correlation of experimental values and predicted from multiple linear regression analysis with DeF yield* as a dependent variable

5. Conclusions

The Rh/zeolite catalyst synthesized in this study was effective for the defluorination of fluorobenzene but had limitations on perfluoroalkyl groups such as trifluoromethyl and pentafluoroethyl. In the presence of difluoromethyl, the reactivity tended to decrease compared to fluorobenzene, but the reaction rate increased significantly when the molecule had a para position like 1,4DFMB. It was difficult to find a consistent trend for all the fluoroarenes experimented in this study, and it seemed that factors related to several of fluoroarene's characteristics were intertwined.

Two multiple linear regression models were obtained for $Log(k_{obs})$ with R^2 of 0.795 and DeF yield* with R^2 of 0.816. In the regression model for the rate constant, since the dependent variable was log scale, the error corresponding to 1 on the graph was an error of 10 times in the actual reaction rate constant. On the other hand, the regression model for DeF yield* was derived without changing the scale of the dependent variable, so it was judged that a more accurate interpretation of the reaction would be possible than $Log(k_{obs})$. The factors that commonly affected the two dependent variables were (1) electron affinity, (2) $\sigma_{position}$, and (3) No.F. For DeF yield*, a total of five variables were selected by adding (4) BDE and (5) Boiling point. Among them, electron affinity had the greatest effect on both the $Log(k_{obs})$ and DeF yield*, and the reaction rate and defluorination rate were lower when the electron affinity was higher. Similarly, $\sigma_{position}$ had a negative effect, but its influence on $Log(k_{obs})$ was relatively low

compared to DeF yield*. BDE appeared to be a significant variable only in DeF yield*. In other words, the strength of C−F bond was more influential for the final DeF yield rather than the reaction rate. Boiling point as a significant variable in DeF yield* regression was expected to influence indirectly on the reaction, such as the coordination between the target substance and the rhodium particle on the catalyst.

In conclusion, the Log(k_{obs}) and DeF yield* cannot be explained in the same way, and the variables tried in this study were more suitable for predicting DeF yield*. The characteristics of catalyst and the binding force of rhodium−fluoroarene, which were not covered in this study, also could affect on the defluorination reaction of fluoroarene, and the coordination between reactants and metals needs to be further studied.

Appendix

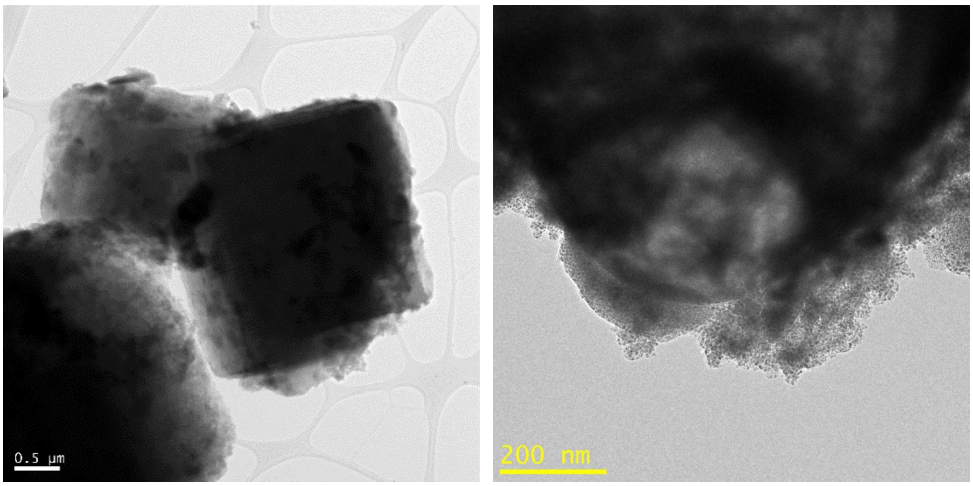

Figure A.1 TEM images of Rh/zeolite catalyst

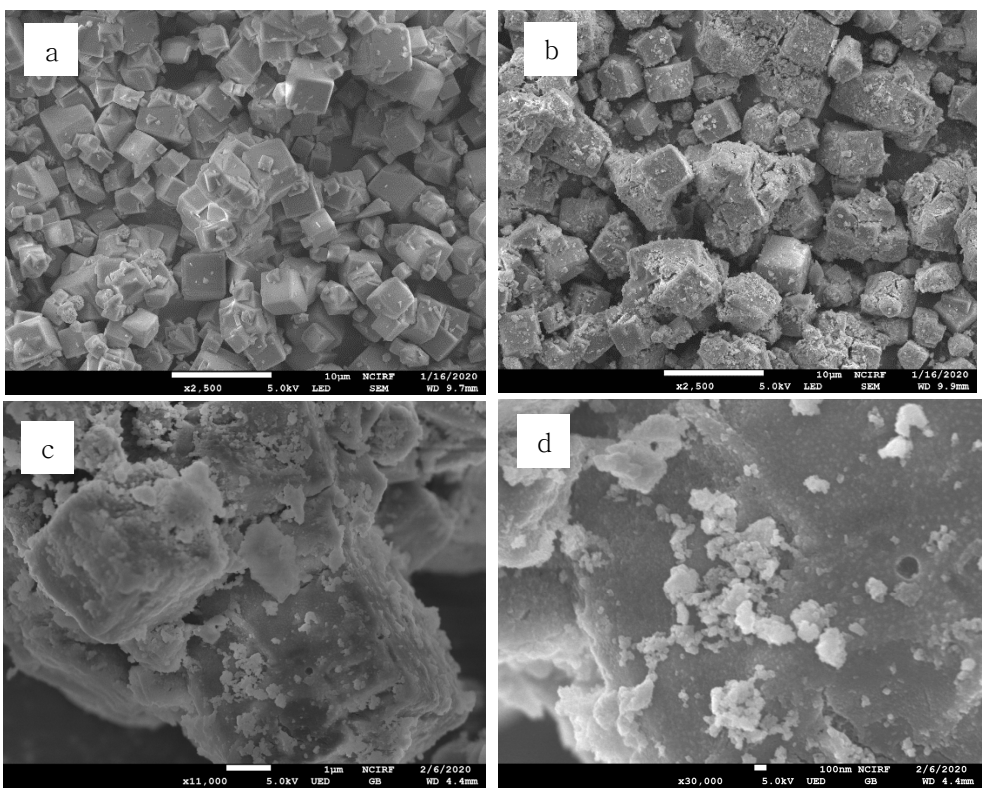

Figure A.2 SEM images of zeolite and Rh/zeolite catalyst (a: zeolite3A, b, c, d: Rh/zeolite)

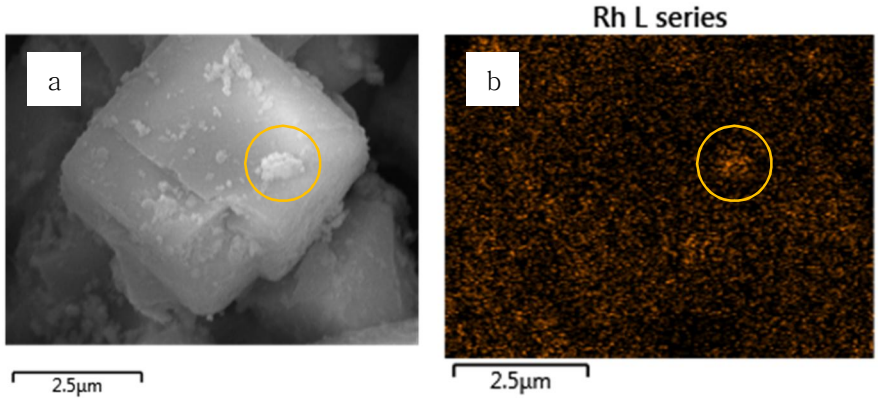

Figure A.3 SEM EDS of Rh/zeolite (a: Electron image, b: atomic mappings)

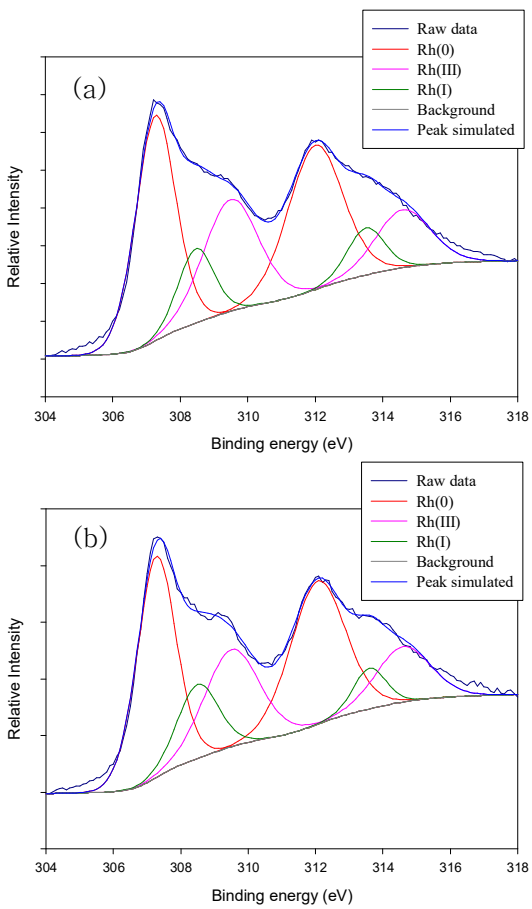

Figure A.4 XPS spectra of (a) Rh/zeolite before reaction and (b) Rh/zeolite catalyst collected after the reaction of penatfluoroethylbeznene[25,26]

Table A.1 SPARC physical and chemical properties calculator statistical performance versus observations[27]

Property	Units	Total# molecule	RMS	R^2	Reaction conditions Temp/Solvent
Vapor pressure	Log atm	747	0.15	0.994	25
Boiling point	℃	4000	5.71	0.994	25
Solubility	Log MF	647	0.40	0.987	25, 41 solvents
Electron affinity	eV	260	0.14	0.98	Gas

Figure A.5 Scatter diagram matrix for all variables

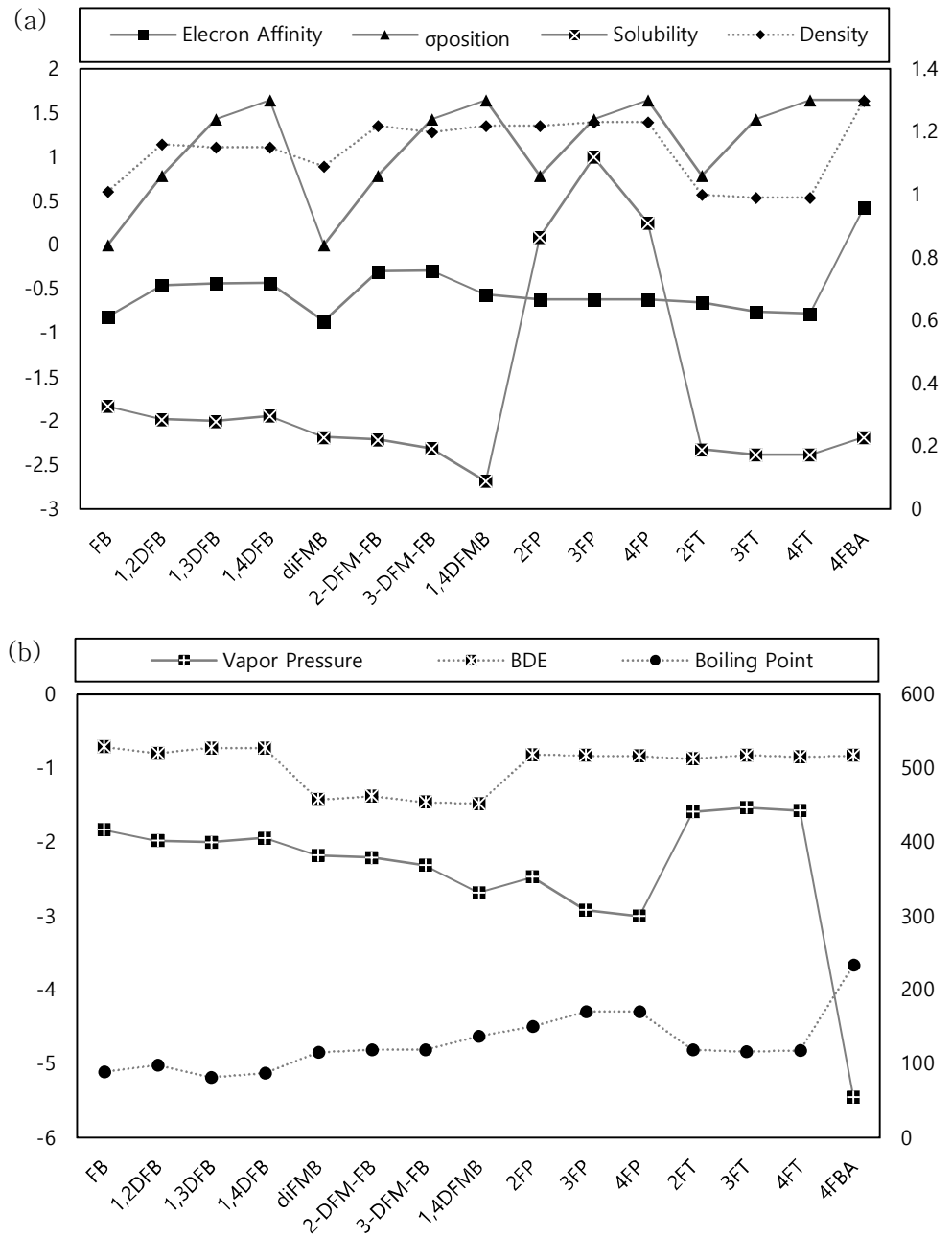

Figure A.6 The calculated values by SPARC and GAMESS (Straight line; left axis, Dotted line; right axis)

Table A.2 Results of ANOVA test and coefficients from multiple linear regression analysis with Log(k_{obs}) as a dependent variable and all chemical properties as independent variables

Model Summary					
R	R^2		Std. Error of The Estimate	Dubin−Watson	
0.924	0.853		0.444766	2.270	
ANOVA					
	Sum of squares	df	Mean square	F	Sig.
Regression	8.106	8	1.013	4.583	0.040
Residual	1.327	6	0.221		
Total	9.433	14			
Coefficients					
	Coefficient	t	Sig.	VIF	
(Constant)	−20.157	−1.743	0.132		
Electron Affinity	−3.309	−2.201	0.070	14.264	
$\sigma_{position}$	−0.670	−1.968	0.097	2.464	
BDE	0.016	1.252	0.257	8.737	
Vapor pressure	0.306	0.513	0.627	21.021	
Boiling point	0.011	0.810	0.440	18.722	
Solubility	−0.537	−1.033	0.341	21.811	
Density	6.570	0.817	0.445	43.537	
No.F	0.427	0.631	0.551	26.840	

Table A.3 Results of ANOVA test and coefficients for multiple linear regression analysis with DeF yield* as a dependent variable and all chemical properties as independent variables

Model Summary					
R	R^2		Std. Error of The Estimate	Durbin−Watson	
0.932	0.869		0.125409	2.016	
ANOVA					
	Sum of squares	df	Mean square	F	Sig.
Regression	0.625	8	0.078	4.964	0.033
Residual	0.094	6	0.016		
Total	0.719	14			
Coefficients					
	Coefficient	t	Sig.	VIF	
(Constant)	−7.397	−2.301	0.061		
Electron Affinity	−0.962	−2.385	0.054	14.439	
$\sigma_{position}$	−0.277	−3.075	0.022	2.423	
BDE	0.009	2.619	0.040	8479	
Vapor pressure	0.197	1.232	0.264	21.289	
Boiling point	0.008	2.208	0.069	18.168	
Solubility	−0.111	−0.800	0.454	22.028	
Density	2.310	1.083	0.321	43.116	
No.F	0.149	0.866	0.420	24.434	

Bibliography

1. Whittlesey, M. K. & Peris, E. Catalytic hydrodefluorination with late transition metal complexes. *ACS Catal.* **4**, 3152–3159 (2014).
2. Key, B. D., Howell, R. D. & Criddle, C. S. Fluorinated organics in the biosphere. *Environ. Sci. Technol.* **31**, 2445–2454 (1997).
3. Sabater, S., Mata, J. A. & Peris, E. Hydrodefluorination of carbon–fluorine bonds by the synergistic action of a ruthenium–palladium catalyst. *Nat. Commun.* **4**, 1–7 (2013).
4. Xu, Y., Ma, H., Ge, T., Chu, Y. & Ma, C. A. Rhodium–catalyzed electrochemical hydrodefluorination: A mild approach for the degradation of fluoroaromatic pollutants. *Electrochem. commun.* **66**, 16–20 (2016).
5. Stanger, K. J. & Angelici, R. J. Hydrodefluorination of fluorobenzene catalyzed by rhodium metal prepared from [Rh(COD)2]+BF4− and supported on SiO2 and Pd−SiO2. *J. Mol. Catal. A Chem.* **207**, 59–68 (2004).
6. Baumgartner, R. & McNeill, K. Hydrodefluorination and hydrogenation of fluorobenzene under mild aqueous conditions. *Environ. Sci. Technol.* **46**, 10199–10205 (2012).
7. Belisle, J. Organic Fluorine in Human Serum: Natural Versus Industrial Sources. *Science (80−.).* **212**, 1509–1510 (1981).
8. Baumgartner, R., Stieger, G. K. & McNeill, K. Complete hydrodehalogenation of polyfluorinated and other polyhalogenated benzenes under mild catalytic conditions. *Environ. Sci. Technol.* **47**, 6545–6553 (2013).
9. Chambers, R. D. *Fluorine in Organic Chemistry*. *Fluorine in Organic Chemistry* (Wiley–Blackwell, 2009). doi:10.1002/9781444305371.

10. Cui, B., Jia, S., Tokunaga, E. & Shibata, N. Defluorosilylation of fluoroarenes and fluoroalkanes. *Nat. Commun.* **9**, 1–8 (2018).
11. Engesser, K.-H., Schmidt, E. & Knackmuss, H.-J. Adaptation of Alcaligenes eutrophus B9 and Pseudomonas sp. B13 to 2-Fluorobenzoate as Growth Substrate. *Appl. Environ. Microbiol.* **39**, 68–73 (1980).
12. Engesser, K.H. & Schulte, P. Degradation of 2-bromo-, 2-chloro- and 2-fluorobenzoate by Pseudomonas putida CLB 250. *FEMS microbioloy Lett.* **60**, 143–147 (1989).
13. Carvalho, M. F., Ferreira, M. I. M., Moreira, I. S., Castro, P. M. L. & Janssen, D. B. Degradation of fluorobenzene by Rhizobiales strain F11 via ortho cleavage of 4-fluorocatechol and catechol. *Appl. Environ. Microbiol.* **72**, 7413–7417 (2006).
14. Holleman, A. F. *Lehrbuch der Anorganischen Chemie*. (Water de Gruyter, 2019).
15. Nova, A., Mas-Ballesté, R. & Lledós, A. Breaking C-F bonds via nucleophilic attack of coordinated ligands: Transformations from C-F to C-X bonds (X= H, N, O, S). *Organometallics* **31**, 1245–1256 (2012).
16. Kuehnel, M. F., Lentz, D. & Braun, T. Synthesis of fluorinated building blocks by transition-metal-mediated hydrodefluorination reactions. *Angew. Chemie - Int. Ed.* **52**, 3328–3348 (2013).
17. Amii, H. & Uneyama, K. C-F bond activation in organic synthesis. *Chem. Rev.* **109**, 2119–2183 (2009).
18. Pike, S. D., Crimmin, M. R. & Chaplin, A. B. Organometallic chemistry using partially fluorinated benzenes. *Chem. Commun.* **53**, 3615–3633 (2017).
19. Schwarzenbach, R. P., Gschwend, P. M. & Imboden, D. M.

Environmental Organic Chemistry. (John Wiley & Sons, 2016).

20. Roberts, A. L., Jeffers, P. M., Wolfe, N. L. & Gschwend, P. M. Structure–Reactivity Relationships in Dehydrohalogenation Reactions of Polychlorinated and Polybrominated Alkanes. *Crit. Rev. Environ. Sci. Technol.* **23**, 1–39 (1993).
21. Blanksby, S. J. & Ellison, G. B. Bond dissociation energies of organic molecules. *Acc. Chem. Res.* **36**, 255–263 (2003).
22. Uyanık, G. K. & Güler, N. A Study on Multiple Linear Regression Analysis. *Procedia – Soc. Behav. Sci.* **106**, 234–240 (2013).
23. Zhan, C. G., Nichols, J. A. & Dixon, D. A. Ionization potential, electron affinity, electronegativity, hardness, and electron excitation energy: Molecular properties from density functional theory orbital energies. *J. Phys. Chem. A* **107**, 4184–4195 (2003).
24. Higashino, S., Saeki, A., Okamoto, K., Tagawa, S. & Kozawa, T. Formation and decay of fluorobenzene radical anions affected by their isomeric structures and the number of fluorine atoms. *J. Phys. Chem. A* **114**, 8069–8074 (2010).
25. Yin, X. *et al.* Behavior, mechanism, and equilibrium studies of rhodium(i) extraction from hydrochloric acid with HMImT. *New J. Chem.* **41**, 10054–10061 (2017).
26. Padeste, C., Cant, N. W. & Trimm, D. L. Reactions of ceria supported rhodium with hydrogen and nitric oxide studied with TPR/TPO and XPS techniques. *Catal. Letters* **28**, 301–311 (1994).
27. Hilal, S. & Karickhoff, S. Verification and validation of the SPARC model. *US Environ.* 44 (2003).

초록

Rh-zeolite 촉매를 이용한 불화 방향족 탄화수소의 환원처리

-화학적 구조가 환원반응상수 및 탈불화에 미치는 영향 규명-

서울대학교 대학원
건설환경공학부
안 선 영

본 연구에서는 화학 산업의 큰 부분을 차지하고 있는 플루오로아렌(fluoroarene) 을 Rh 촉매를 이용하여 환원 처리하는 실험을 수행하였다. 로듐 촉매는 C-H 결합에 대한 C-F 결합을 감소시킬 수 있으며, 따라서 Rh/zeolite 촉매를 합성하여 다양한 구조의 플루오로아렌을 감소시켰다. 실험 대상 물질로 fluorobenzene, difluorobenzene, (difluoromethyl)benzene, (trifluoromethyl)benzene, (pentafluoroethyl)benzene, fluorophenol, fluorotoluene, fluorobenzoic acid 를 선정하여 물질 별 반응속도와 탈불화율을 비교하였다. 반응속도 상수 k_{obs}는 log 를 취하여 변환하고, 탈불화율(defluorination yield; DeF yield) 는 플루오린의 수로 표준화 하여 각 물질들의 반응성과 탈불화 정도를 비교하였다. fluorobenzene과 difluorobenzene 계열 (1,2-difluorobenzene, 1,3-difluorobenzene, 1,4-difluorobenzene) 에서는 작용기가 1개일 때, 2개일 때 ortho, meta, para 순서로 반응속도가 감소하는 결과를 얻었고, 이는 다른 논문들의 결과와 일치하는 결과였다. 그러나 trifluoromethyl, pentafluoroethyl과 같이 perfluoroalkyl에 대해서는 반응이 일어나지 않거나 탈불화율이 30% 이하로 낮게 나타나 과불화 알킬 구조에서는

Rh 촉매 적용에 한계가 있었다.

반응이 일어나지 않거나 탈불화 반응이 잘 일어나지 않았던 물질 ((trifluoromethyl)benzene, 4-trifluoromethylphenol, (pentafluoroethyl)-benzene) 을 제외한 플루오로아렌에 대하여 이들의 구조적 특징이 반응속도 및 탈불화율에 어떤 영향을 미쳤는지 알기 위해 다중회귀분석을 수행하였다. 다중회귀분석을 수행하기 위해서는 2개 이상의 독립변수가 필요했으며, 각 플루오로아렌의 구조적 특징을 대표할 수 있는 변수를 선정하였다. 본 연구에서 독립변수로는 $\sigma_{position}$, Bond dissociation energies (BDE), 불소의 수 (No.F) 그리고 SPARC를 통해 계산한 물질의 화학적 특성값들이 선정되었고, 이 독립변수들을 조합하여 적용하면서 다중회귀분석을 수행하였다. 그 결과 반응속도상수 ($Log(k_{obs})$) 에는 전자친화도 (electron affinity), $\sigma_{position}$, and No.F 가 유의미한 영향이 있었고, 탈불화율 (DeF yield*) 에는 전자친화도, $\sigma_{position}$, BDE, 끓는점 (boiling point), No.F 가 유의미한 영향이 있는 것으로 나타났다. 각각의 회귀모델의 R^2 값은 $Log(k_{obs})$에 대해 0.795, DeF yield*에 대해 0.816 이었으며, 본 연구에서 선정한 변수들로 회귀모델을 적용하였을 때 반응속도보다 탈불화율의 경향을 더 잘 설명할 수 있다는 결론을 얻었다. 즉, 플루오로아렌의 구조적, 화학적 특성은 반응속도보다 최종 탈불화율에 더 큰 영향을 미친다는 것이다. 이는 로듐 촉매에 의해 탈불화반응 뿐만 아니라 수소화반응 (hydrogenation) 또한 함께 일어나고 플루오로아렌의 구조적, 화학적 특성이 탈불화/수소화 반응의 비율을 변화시킬 수 있음을 시사한다.

수소화반응을 통해 생성될 수 있는 중간생성물질의 조합은 매우 많기 때문에 모두 정량할 수는 없었으나, 1-difluoromethyl-2-fluorobenzene 과 1-difluoromethyl-3-fluorobenzene 을 시작물질로 실험하였을 때 예상되는 중간생성물질로

difluoromethylbenzene, fluorotoluene, toluene, methylcyclohexane을 선정하여 반응 시간에 따라 농도를 정량하였다. 그 결과 두 경우 모두 초기 농도 대비 dimethylbenzene과 fluorotoluene의 농도 비율이 매우 낮게 측정되었으며 생성된 시간도 비슷한 수준으로 나타났다. 즉, 벤젠고리에 결합된 불소나 dimethyl의 불소 모두 빠른 속도로 탈불화 반응이 일어날 수 있었으며, 최종 탈불화율의 차이는 불소가 제거되지 않은 채로 수소화반응이 일어난 물질이 생성되었을 가능성이 있다. 이러한 현상은 1,3-difluorobenzene, 1-difluoromethyl-3-fluorobenzene, and 3-fluorophenol 과 같이 두 작용기가 meta 위치에 있을 때 발생하였으며, 3-fluorotoluene에서는 예외였다.

따라서 다양한 구조의 Fluoroarene의 경우 제거 속도와 탈불화율의 경향성은 각각 다른 방식으로 접근하여 처리 효율을 예측할 수 있을 것이며, 기존의 linear chain 구조를 가진 PFCs와는 다른 접근이 필요하다.

주요어: 플루오로아렌, 탈불화반응, 로듐 촉매, 구조-반응 관계식

학번: 2018-26687

공학석사 학위논문

Reductive treatment of fluoroarenes using zeolite supported Rh-based catalyst

-Elucidating influence of chemical structure on reduction rate and defluorination-

Rh-zeolite 촉매를 이용한 불화 방향족 탄화수소의 환원처리

-화학적 구조가 환원반응상수 및 탈불화에 미치는 영향 규명-

2020년 8월

서울대학교 대학원

건설환경공학부

안 선 영

Reductive treatment of fluoroarenes using zeolite supported Rh-based catalyst

-Elucidating influence of chemical structure on reduction rate and defluorination-

지도교수 최 정 권

이 논문을 석사 학위논문으로 제출함

2020 년 8 월

서울대학교 대학원

건설환경공학부

안 선 영

안선영의 석사 학위논문을 인준함

2020 년 8 월

위 원 장 김 재 영 (인)

부위원장 최 정 권 (인)

위 원 최 용 주 (인)

Abstract

Reductive treatment of fluoroarenes using zeolite supported Rh-based catalyst

- Elucidating influence of chemical structure on reduction rate and defluorination-

Seonyoung An
Civil and Environmental Engineering
The Graduate School
Seoul National University

This study used zeolite supported Rh-based catalyst and hydrogen as a reductant to reduce fluoroarene, which is also a big part of the chemical industry. Rh/zeolite catalyst was applied for the reductive treatment of fluoroarenes with various structures. The experimented fluoroarenes were fluorobenzene, difluorobenzene, (difluoromethyl)benzene, (trifluoromethyl) -benzene, (pentafluoroethyl) benzene, fluorophenol, fluorotoluene, fluorobenzoic acid, and their pseudo-first-order reaction constant and defluorination yield were compared with each other. The reaction rate of fluorobenzene and difluorobenzene decreased in the order of one substituent (fluorobenzene), ortho (1,2-difluorobenzene), meta (1,3-difluorobenzene), and para (1,4-difluorobenzene). It was the same as the results of other papers. However, perfluoroalkyl groups,

such as trifluoromethyl and pentafluoroethyl, did not react or the defluorination yield was lower than 30%, so the application of Rh catalyst had a limitation in the perfluorinated alkyl structure.

Multiple linear regression analysis was performed to elucidate the effect of structural characteristics of each fluoroarenes on their reaction constants and defluorination yield, except for (trifluoromethyl)benzene, 4-trifluoromethylphenol, (pentafluoroethyl)benzene. To perform multiple linear regression analysis, two or more independent variables were required, and variables capable of representing the structural characteristics of each fluoroarene were selected, such as $\sigma_{position}$, bond dissociation energies (BDE), number of fluorine (No.F), and some chemical properties calculated by SPARC chemical calculator. As a result, the electron affinity, $\sigma_{position}$, and No.F had a significant effect on the reaction rate constant ($Log(k_{obs})$), and the electron affinity, $\sigma_{position}$, BDE, boiling point, and No.F was found to have a significant effect on defluorination yield (DeF yield*). The R^2 value of each regression model was 0.795 for $Log(k_{obs})$ and 0.816 for DeF yield*. Thus, the regression model for defluorination yield was better explained than for the reaction rate constant. In other words, the structural and chemical properties of fluoroarene had a greater effect on the final defluorination yield than the reaction rate. It suggested that not only the defluorination reaction but also hydrogenation occurred by Rh/zeolite catalyst, and the structural and chemical properties of fluoroarene can change the ratio of defluorination/hydrogenation reaction.

Since there were expected to be various intermediates that can be produced through hydrogenation reaction, some of the expected intermediates were quantified when 1-difluoromethyl-2-fluorobenzene and 1-difluoromethyl-3-fluorobenzene were experimented as starting materials. Difluoromethylbenzene, fluorotoluene, toluene, and methylcyclohexane were selected as the expected intermediates, and the concentration was quantified according to the reaction time. As a result, in both cases, the concentration ratio of dimethylbenzene and fluorotoluene compared to the initial concentration was measured very low, and the generated time was similar. In other words, both fluorine attached to the benzene and fluorine of dimethyl could be rapidly defluorinated, and it was suspected that unknown intermediates, which undergo only hydrogenation, not defluorination, might be generated. This phenomenon occurred when two functional groups were in the meta position, such as 1,3-difluorobenzene, 1-difluoromethyl-3-fluorobenzene, and 3-fluorophenol, except for 3-fluorotoluene.

Keyword: Fluoroarene, Hydrodefluorination, Rhodium catalyst, Structure-reactivity relationships

Student Number: 2018-26687

Table of Contents

Contents of Table

Contents of Figures

1. Introduction

1.1. Study Background

Poly- and per-fluorocarbons (PFCs) are manufactured and used for various purposes such as fire-fighting applications, medicine, cosmetics, lubricants, etc[1]. With increasing industrial use of the fluorochemicals, great attention has been shown to the concern of their impact on human health and fate in the environment[2]. Their strong C-F bonds particularly make them recalcitrant in the water and wastewater treatment processes. Therefore, there have been many studies to remove C-F bonds from PFCs.

Among them, catalytic hydrodefluorination is a promising way to treat PFCs[1,3-5]. While C-F bonds in few fluoroarenes such as fluorobenzene and its congeners are known to be reduced to C-H bond in the presence of alumina-supported Rh catalyst[4-6]. However, the applicability of Rh-based catalyst for poly- and perfluoroalkyl groups was not explored.

In this study, we focused on fluoro-aromatic compounds called fluoroarenes. Fluoroarene is also a big part of the chemical industry, especially in the pharmaceutical, thus it is more likely to have been released into the environment[2]. And even more, for workers handling fluoroarences, the organic fluorine level of 1.0-71 ppm have been reported in their blood serum[7]. However, little is known of fluoroarenes having various structures such as fluoromethyl or fluoroethyl groups and their effect on the hydrodefluorination

reaction.

Rebekka and her colleagues found that the reaction rate decreases as the number of fluorine increases and the distance between the substituents increase in the case of the FB series when using Rh-based catalysts[8]. In the case of fluoroarene with a fluoromethyl or fluoroethyl group, it has limitations to test the activity of the catalyst in all cases, because there are too many combinations of each substituent and new fluoroarenes are continuously being produced. Therefore, this study was planned with the expectation that the reactivity of newly synthesized fluoroarene can be predicted by knowing how some basic type or position of fluorine substituent affects the compound reactivity.

1.2. Purpose of Research

The objective of this research is to elucidate the effect of basic fluorine substituent on the reactivity of fluoroarenes, thus predicting the reactivity and defluorination yield of the reaction.

1) Investigate the influence of chemical structure on the removal rate and defluorination yield of fluoroarenes using a Rh/zeolite catalyst
2) Determine structure-reactivity relationships of catalytic reduction of fluoroarenes, and quantify the effect of each substituent.

1.3. Research area

In this study, hydrodefluorination of fluoroarenes was carried out using a zeolite-supported Rh catalyst and H_2 as a reductant under mild aqueous conditions.

1) Various fluorine substituents (fluorine, difluoromethyl, trifluoromethyl, pentafluoroethyl), functional groups (hydroxyl, methyl, carboxylic acid) and their position (one substituent, ortho, meta, para) were dealt with.
2) The pseudo-first-order reaction constant, defluorination yield, and defluorination ratio were calculated to show the reactivity of each fluoroarenes.
3) The relationship between structural properties and reactivity of each fluoroarenes was quantified through multiple regression analysis.

2. Literature review

2.1. Fluoroarene

Fluoroarene means any fluoro-derivative of arene, for example, fluorobenzene, hexafluorobenzene, fluorophenol, and is also called fluoroaromatic. Fluoroarene is used for many purposes such as pharmaceuticals, plant protection agents (herbicides, fungicides), surfactants, refrigerants, intermediates in organic synthesis, and solvents[2]. Even in 1992, it was estimated that businesses involving the sale of compounds containing carbon-fluorine bonds were worth about $ 50 billion per year, and have been growing ever since[9]. Moreover, a SciFinder Search revealed that fluoroarenes are the largest group of commercially available halogenated arenes; the number of registered compounds is as follows; Ar-F (6,336,383), Ar-Cl (6,186,473), Ar-Br (3,407,354), and Ar-I (433,556)[10]. Thus, not surprisingly, significant research efforts have been directed toward C-F cleavage protocols to develop synthetic strategies and so the amount discharged to the environment increased. The compounds gradually accumulate in the environment, reaching concentrations that are hazardous to living organisms[2].

These fluoroarenes are not easily decomposed in the environment. Compared to the relatively activated C-X bonds of halogenated arenes and their equivalents (Ar-X; X=Cl, Br, I), which easily undergo oxidative addition in metal-catalyzed coupling

reactions, the cleavage of C–F bonds in fluoroarenes (Ar–F) is in general significantly more challenging due to their high dissociation energy; they are arguably the strongest bonds that carbon can form (Figure 2.4). They also have a very slow microbial decomposition rate. There have been several studies on the degradation of fluorobenzene and fluorobenzoic acid by bacteria, showing that it takes about 10~45 hours for maximum removal of initial fluoroarene[11–13]. It means that they are strongly resistant to biological degradation and that is why catalytic treatment for the fast decomposition of fluoroarenes has recently been prominent.

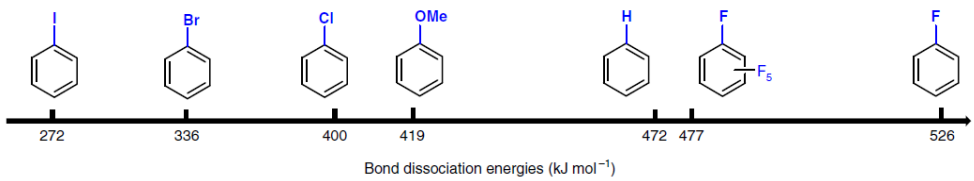

Figure 2.1 Bond dissociation energies (BDE) of halogenated benzenes[10]

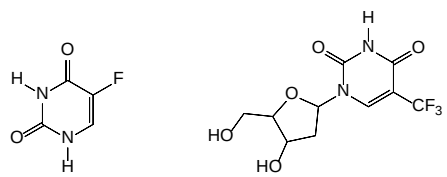

5–Fluorouracil
(anti–cancer)

Trifluridine®
(anti–viral)

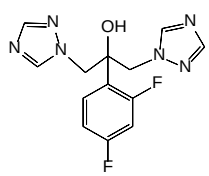

Fluconazole®
(anti–fungal)

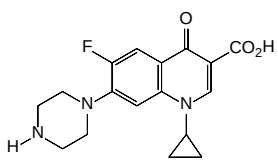

Ciprofloxacin®
(antibacterial)

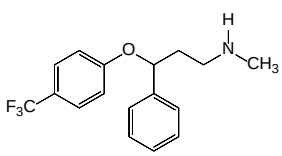

Prozac®
(anti–depressant)

Figure 2.2 Examples of fluorinated pharmaceuticals

2.2. Rhodium catalyst

Rhodium is a highly reactive catalyst on hydrogenation and well known as one of the elements on the three-way catalytic converter for the automobile exhaust gas purification systems. Rhodium catalyst is generally used for hydrogenation and its ability to activate C-F bonds has been attracting attention as a treatment of PFCs has been in the spotlight.

The common oxidation state of rhodium is 3+, but oxidation states from 0 to +6 also exist and hydrodefluorination reaction requires zero-valent Rh(0) which can reduce fluoroarenes. Therefore, to utilize the rhodium catalyst for reduction reaction, the Rh(Ⅲ) should be activated to zero-valent Rh(0), meaning a reduction of rhodium. There are several ways to activate rhodium, such as contacting the $NaBH_4$ solution or flowing hydrogen gas at high temperatures. In this study, hydrogen gas was used for activation of the rhodium when synthesizing zeolite-based rhodium catalysts. The detailed method was described in the method part.

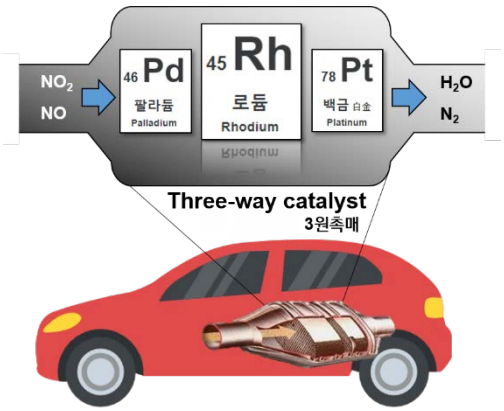

Figure 2.3 Rhodium usage for three-way catalyst in the automobile system

Table 2.1 Oxidation states of rhodium[14]

+0	$Rh_4(CO)_{12}$
+1	$RhCl(PH_3)_2$
+2	$Rh_2(O_2CCH_3)_4$
+3	$RhCl_3$, Rh_2O_3
+4	RhF_4, RhO_2
+5	RhF_5, Sr_3LiRhO_6
+6	RhF_6

2.3. Hydrodefluorination

The most simple C-F bond transformation is hydrodefluorination (HDF) which, shows a surprising mechanistic diversity[9-11]. The reaction formally involves the activation of a carbon-fluorine bond resulted from the introduction of hydrogen to form the hydrogenated products.

The first example of a catalytic HDF reaction was reported by Swarts in 1920, who developed Pt and Ni alloys for the HDF of mono fluorinated arenes using hydrogen gas. However, this method suffers from the inconveniences derived from the need for high temperatures and pressures. Subsequent researchers showed that various transition-metal-mediated catalyst easily cleaves a C-F bond of fluoroarene, such as hexafluorobenzene (C_6H_6), in mild condition[3,5,8,18]. When using a Rh/Al_2O_3-based heterogeneous

catalyst under mild condition (room temperature, 1 atm H_2), the observed fluorinated intermediates indicate that adjacent fluorine substituents are removed preferentially[8].

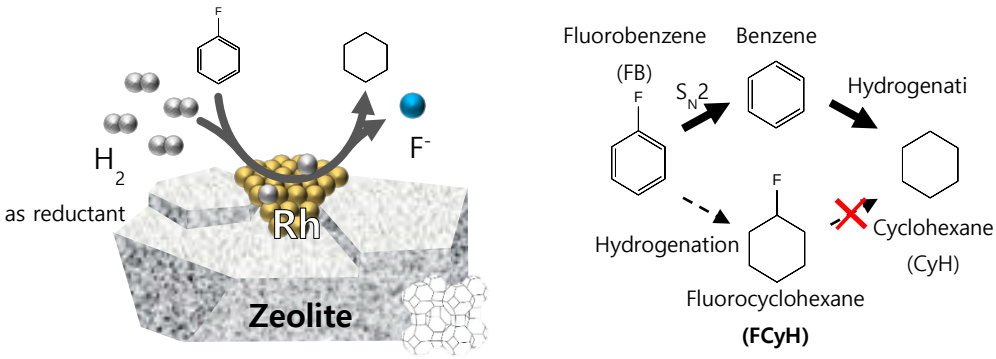

Figure 2.4 Reactions of fluorobenzene with H_2 catalyzed by rhodium catalyst[5]

2.4. Structure–reactivity relationships

For many environmental matrices, experimental constants or coefficients required to assess quantitatively the behavior of a given compound are often not available and, therefore, have to be estimated. In these approaches, one tries to express the free energy of a given in the system of interest by one or several other known free energy terms in a way that they are linearly related. Such approaches are called linear free energy relationships (LFERs). They are useful for predictive purposes and also helpful for checking reported experimental data for consistency[19].

For example, Hammett(1940) found that for substituted benzoic acid the effect of substituents in either the meta or para position on

the standard free energy change of the carboxyl group's dissociation could be expressed as the sum of the free energy change of the dissociation of the unsubstituted compound and the combination of various substituents[19]. As shown in Figure 2.3, plotting $pK_{aH}-pK_a$ values for *meta*- and *para*-substituted phenylacetic acids versus $\sum\sigma_j$ values results in a straight line with a slope, ρ, which is a measure of how sensitive the dissociation reaction is to substitution as compared with substituted benzoic acid. $\sum\sigma_j$ represents the sum of the inductive effect of the compounds.

The Hammett equation, however, does not appear to have been successfully applied to hydrodefluorination reactions of fluoroarenes in aqueous solution. One difficulty in using it relates to the question of an appropriate reference compound. Unsubstituted compounds are generally selected as reference compounds, but non-fluorinated compounds do not undergo defluorination. Correlation can be performed without normalizing reactivity to some reference compound; a further complication, however, is that some substrates undergo base-prompted reaction, whereas reaction rates of other compounds are independent of pH[20]. Therefore, in this study, solution pH 7 was kept in the kinetic experiment to exclude the base-prompted reaction, and multiple linear regression analysis was conducted using non-normalized reactivity and chemical properties of the target materials.

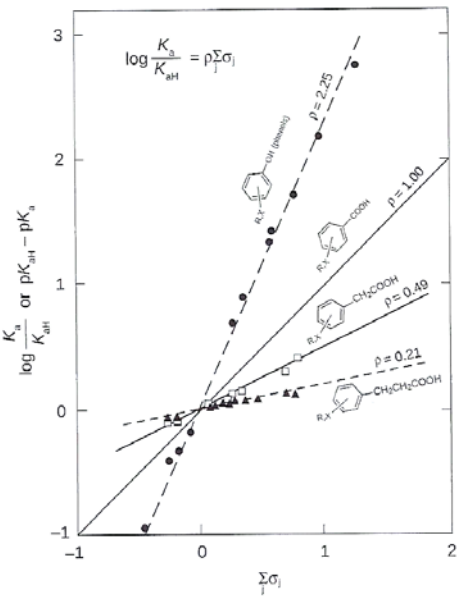

Figure 2.5 Hammett plot for meta- and para-substituted phenols, phenylacetic acids, and 3-phenylpropionic acids; data from Serjeant and Dempsey (1979)[19].

Table 2.2 Hammett constant for some common substituents; data from Dean (1985) and Shorter (1994 and 1997)[19].

Substituent j	σ_{jmeta}	σ_{jpara}	Substituent j	σ_{jmeta}	σ_{jpara}	σ^{-}_{jpara}
– H	0.00	0.00	– OH	0.10	–0.36	
– CH_3	–0.06	–0.16	– OCH_3	0.11	–0.24	–0.12
– CH_2CH_3	–0.06	–0.15	– $OCOCH_3$	0.36	0.31	
– $CH_2CH_2CH_2CH_2$	–0.07	–0.16	– CHO	0.36	0.22	1.03
– $C(CH_3)_3$	–0.10	–0.20	– $COCH_3$	0.38	0.50	0.82
– $CH=CH_2$	0.08	–0.08	– $COOCH_3$	0.33	0.45	0.66
– C_6H_5 (phenyl)	0.06	0.01	– CN	0.62	0.67	0.89
– CH_2OH	0.07	0.08	– NH_2	–0.16	–0.66	
-– CH_2Cl	0.12	0.18	– $NHCH_3$	–0.25	–0.84	
– CCl_3	0.40	0.46	– $N(CH_3)_2$	–0.15	–0.83	
– CF_3	0.44	0.57	– NO_2	0.73	0.78	1.25
– F	0.34	0.05	– SH	0.25	0.15	
– Cl	0.37	0.22	– SCH_3	0.13	0.01	
– Br	0.40	0.23	– $SOCH_3$	0.50	0.49	
– I	0.35	0.18	– SO_2CH	0.68	0.72	
			– SO_3^-	0.05	0.09	

Furthermore, among various variables that can represent the chemical structure, bond dissociation energies (BDE) have been used to describe various chemical transformations as variables to interpret bond strength. The definition of BDE is as follows; BDE for a bond R−F that is broken through the reaction

$$RF \rightarrow R\bullet + \bullet F$$

is defined as the standard−state enthalpy change for the reaction at a specified temperature, here at 298 K.

$$BDE = \Delta Hf_{298} = \Delta Hf_{298}(R\bullet) + \Delta Hf_{298}(\bullet F) - \Delta Hf_{298}(RF)$$

Using these ideas, it is possible to determine the energetics of a wide range of simple but important reactions involving the exchange of a single bond[21]. In this study, BDE of C−F bonds in fluoroarene were calculated based on density functional theory (DFT) for using them as structural variables.

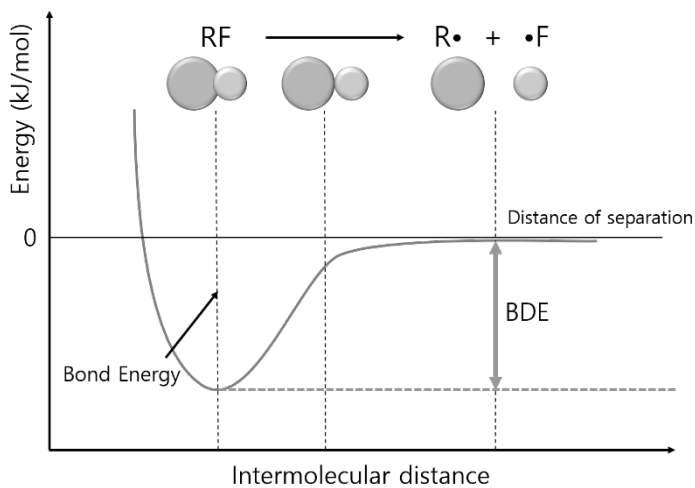

Figure 2.6 Definition of bond dissociation energies (BDE)

2.5. Multiple linear regression analysis

Regression analysis is a statistical technique for estimating the relationship among variables that have reason and result relations. Regression models with one dependent variable and more than one independent variable are called multiple linear regression[22]. In this study, data for multiple linear regression analysis was prepared from the kinetic experiments and computational calculations, which were described in the method part.

Multiple linear regression analysis models are formulated as in the following;

$$y = \beta_0 + \beta_1 x_1 + \beta_2 x_2 + \cdots + \beta_n + \varepsilon$$

y = dependent variable

x_i = independent variable

β_i = parameter

ε = error

The assumption of multiple linear regression analysis is normal distribution, linearity, freedom from extreme values, and having no multiple ties between independent variables.

3. Materials and methods

3.1. Reagents

Hydrogen (99.999%) and nitrogen (99.999%) gas were purchased from Daehan Gas Company (Republic of Korea). Fluorobenzene, (difluoromethyl) benzene, 1,4-difluorobenzene, benzene, 4-trifluoromethylphenol, (trifluoromethyl)benzene, methanol (for HPLC, ≥ 99.9%), dichloromethane, sodium carbonate, sodium bicarbonate, and rhodium(Ⅲ) nitrate hydrate were purchased from Sigma-Aldrich. 1,2-Difluorobenzene, 1,3-difluorobenzene, 1,4-difluorobenzene, 1-difluoromethyl-2-fluorobenzene, 1-difluoromethyl-3-fluorobenzene, 1,4-bis(difluoromethyl)Benzene, 2-fluorophenol, 3-fluorophenol , 4-fluorophenol, 2-fluorotoluene, 3-fluorotoluene, 4-fluorotoluene, 4-fluorobenzoic acid, methylcyclohexane, hexanes (mixed isomers, 60+% n-hexane), and ethyl acetate were purchased from Alfa Aesar. Fluorocyclohexane was purchased from Acros-Organics. Potassium phosphate monobasic, potassium phosphate dibasic anhydrous were purchased Daejung Chemicals & Materials Company.

3.2. Catalyst

The catalyst was prepared with supports zeolite 3A (Wako Pure Chem. Ind. Ltd) as a sieve of 0.34−0.75 μm of particles. Incipient impregnation wetness method was used and the desired rhodium loading was 4 wt%. Rhodium nitrate solution containing an appropriate amount of rhodium was added dropwise to zeolite 3A, mixed and dried overnight in the oven (60 ℃). After completely dried, the powder was thermos−treated to reduce Rh(Ⅲ) to zero−valent Rh(0) by flowing hydrogen gas at high temperature using a tube furnace. Temperature profile for the tube furnace is:

1) Nitrogen: 25 ℃ (room temperature), ramp 20min to 120 ℃, hold 30 min, cooling 30 min
2) Hydrogen: 25 ℃ (room temperature), ramp 40 min to 200 ℃, hold 20 min, ramp 20 min to 400 ℃, hold 120 min, cooling 60 min

The catalyst was stored in a sealed container with silica gel, and no special precautions were taken to avoid exposure to air prior to the batch experiments. The Rh loading rate of 4.1 wt% was measured by the acid extraction method with ICP−OES. Rhodium distributions in the catalyst were examined by field emission transmission electron microscope (FE−TEM, JEM−F200) with a 200 kV acceleration voltage. X−ray photoelectron spectroscopy (XPS) was used to confirm that the rhodium charge state was simultaneously present in trivalent and zero−valent and stable at room temperature. TEM, SEM images, XPS spectra were shown in the Appendix.

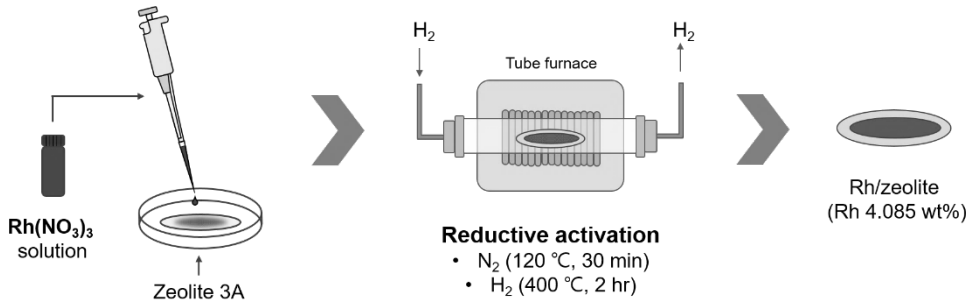

Figure 3.1 Synthesis of Rh/zeolite catalyst and reductive activation method

Table 3.1 Chemical structure of the fluoroarenes used in this study and their abbreviations

Structure	Name/Abbreviations	Structure	Name/Abbreviations
	Fluorobenzene FB	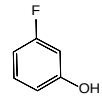	3-Fluorophenol 3FP
	1,2-Difluorobenzene 1,2DFB	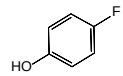	4-Fluorophenol 4FP
	1,3-Difluorobenzene 1,3DFB		2-Fluorotoluene 2FT
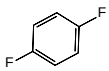	1,4-Difluorobenzene 1,4DFB		3-Fluorotoluene 3FT
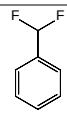	(Difluoromethyl)benzene DFMB	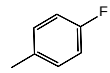	4-Fluorotoluene 4FT
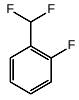	1-Difluoromethyl-2-fluorobenzene DFM-2FB	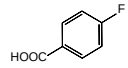	4-Fluorobenzoic acid 4FBA
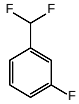	1-Difluoromethyl-3-fluorobenzene DFM-3FB	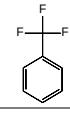	(Trifluoromethyl)benzene TFMB
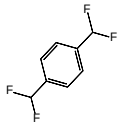	1,4-Bis(difluoromethyl)benzene 1,4DFMB	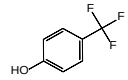	4-(Trifluoromethyl)phenol 4TFMP
	2-Fluorophenol 2FP		(Pentafluoroethyl)benzene PFEB

3.3 Batch experiments

A mixture of phosphate buffer (pH 7, 10 mM, 99 mL), Rh/zeolite catalyst (0.1g/L) in a 120 mL serum bottle was stirred using an electronic magnetic stirrer in a water bath (20±2 ℃) for 30 min to allow the catalyst to disperse well. Buffer was used to preventing the slight increase in pH observed in the un-buffered system and shown to not affect the determined rate constants. The solution was purged with H_2 for 5 min prior to initiation of the reaction and kept under 1 atm during the reaction. Starting fluoroarenes (20 mM, 1 mL, dissolved in methanol) was added to the reactor through the septa using glass syringes. Vigorous stirring was continued during the reaction. Batch experiments were performed triplicate for each target fluoroarene.

Aliquots of 0.5 mL were sampled with a glass syringe and added to 3 mL organic solvent in a 4 mL amber vial. The water sample and the organic solvent separated into two layers were mixed vigorously for 1 min using the vortex mixer and allowed to equilibrate for 15-19 hours (overnight) for partitioning into the organic solvent. Due to the efficiency of the extraction, water samples did not require filtration. The organic solvent used for extraction was different depending on the partitioning coefficient of each fluoroarenes, as shown in Table 3.2.

For every control samples, fluoride was not detected, which means there was no reaction by hydrogen without the catalyst.

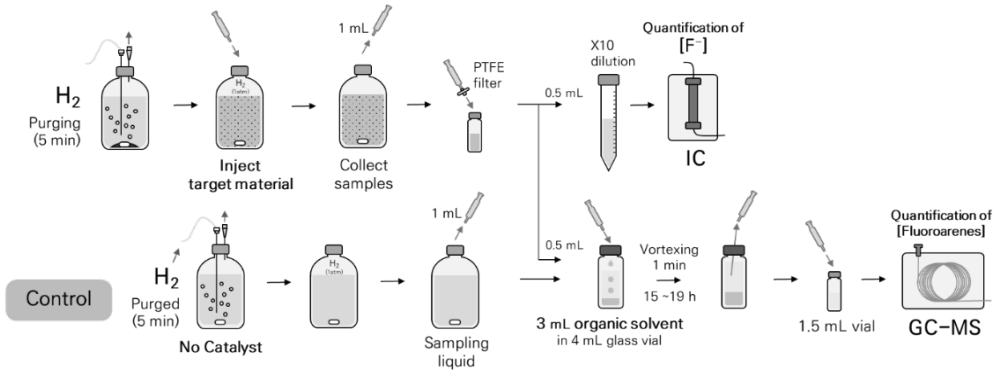

Figure 3.2 Scheme of the kinetic experiment

Table 3.2 Organic solvent for extraction of each fluoroarene

Organic solvent	Hexanes		Dichloromethane	Ethyl acetate	
Fluoroarenes	FB	DFMB	2FP	TFMB	2FT
	1,2DFB	DFM-2FB	3FP	1,4TFMB	3FT
	1,3DFB	DFM-3FB	4FP	PFEB	4FT
	1,4DFB	1,4DFMB		4TFMP	

*4FBA was measured by LC-MS without extraction procedure

3.4 Analytical methods

Benzene, toluene, methylcyclohexane, all fluoroarenes extracted by organic solvents, except fluorobenzoic acid, were analyzed by an Agilent 7890B gas chromatograph (GC) linked to an Agilent 5977B Mass Selective Detector (MSD). The column used was an HP-5MS 5% phenyl methyl silox (30 m × 250 μm × 0.25 μm). Temperature profiles applied were different for fluoroarenes as shown in Table 3.3. Calibration standards were prepared using the same solvent with the extraction solvent for each material. The oven temperature was shortened according to the retention time of the target material.

Agilent 1260 series LC system (Agilent, Waldronn, Germany) coupled with an Agilent 6120 single-quadrupole mass analyzer was used for the analysis of 4-fluorobenzoic acid. The chromatographic runs were carried out on a single Zorbax Extend C18 (2.1 × 150 mm, 1.8 μm) column from Agilent Technologies. Mixtures of acetonitrile (solvent A) and 0.1% formic acid in water (solvent B) were used as the mobile phase eluents. The eluent gradient time profile was as follows: 90% A at t = 0 min, decreased to 20% A from 0 min to 3 min, held at 20% A for 2 min, increased to 90% A from 5 min to 6 min, and re-equilibrated from 6 min to 20 min. The injection volume was 5 μL and the column temperature was set at 40 ℃. The elution flow rate was maintained at 0.2 mL/min. Electrospray ionization MS in the negative mode was used for 4-fluorobenzoic acid. The following MS settings were used: drying gas (i.e., N2) flow rate of 7.0 L/min, nebulizer pressure of 50 psi, drying gas temperature of 350 °C, capillary voltage of 1500 V (positive) and 4500 V (negative), and fragmentor voltages of 100 V.

Ion chromatography (ICS-1100, Thermo Scientific) was used for the analysis of the concentration of fluoride in the bulk samples. The sample was separated on Dionex IonPac AS23 (250 mm × 4.0 mm) column with 4.5 mM Na_2CO_3/$NaHCO_3$ as eluent at a flow rate of 1 mL/min and detected by the suppressed conductivity detector. The detection limits of fluoride were 0.05 mg/L.

Table 3.3 GC Oven temperature profiles applied for fluoroarenes and other arenes

	Temperature profiles	Materials
Method 1	35 ℃ (2 min), ramp (6 ℃/min) to 70 ℃ (3 min)	FB, 1,2DFB, 1,3DFB, 1,4DFB, DFMB, DFM-2FB, DFM-3FB, 1,4DFMB, 2FT, 3FT, 4FT, TFMB, 4TFMP, PFEB, and their intermediates
Method 2	100 ℃ (2 min), ramp (6 ℃/min) to 125 ℃ (3 min)	2FP, 3FP, 4FP, and their intermediates

3.5. Calculation methods

Bond dissociation energies (BDE) were calculated for each fluoroarenes by GAMESS software. The calculation method was M06-2X hybrid functional with an SMD solvation model to consider the polar properties of water molecules around. Geometry optimization with 6-31+G* basis set and single point energy and Hessian calculation with 6-311++G** were performed. All values were given at 298 K by classifying the fluorine directly bound to benzene and fluorine of the difluoromethyl group. The BDE calculation formulas were as below.

$$H^0\ (298K) = E_0 + ZPE + H_{trans} + H_{rot} + H_{vib} + RT$$

$$BDE\ (298K) = H^0\ (R\bullet) + H^0(\bullet F) - H^0\ (RF)$$

ZPE : Zero-point energy, which is the lowest possible energy that a quantum mechanical system may have

Online SPARC chemical calculator was used to obtain physical and chemical properties of fluoroarenes. SPARC uses computational algorithms based on fundamental chemical structure theory to estimate a variety of reactivity parameters. The references were noticed on ARChem (Automated Reasoning in Chemistry). Multiple linear regression analysis for each dependent variables Log(k_{obs}) and DeF yield* was performed by SPSS software.

4. Results and discussions

4.1. Reaction kinetics and defluorination yield

It should be noticed that not only defluorination but also hydrogenation are considered in the removal of target fluoroarenes. In other words, the defluorination reaction needs to be distinguished from the hydrogenation reaction. As conducting the reaction with Rh/zeolite catalyst on targeted fluoroarenes, fluoride was not always generated as much as the proportion of target removed. This result shows that the Rh/zeolite catalyst can reduce not only C−F bonds but also double bonds of benzene rings, so that makes benzene structure to saturated structure like cyclohexane.

4.1.1. Pseudo−first−order reaction constant

Pseudo−first−order kinetics were observed for the degradation of the fluoroarenes. Hydrogen was assumed to be constant and available in excess during the reaction. Pseudo−first−order rate constants (k_{obs}) were obtained by linear regression. Most of the fluoroarenes are removed by more than 90% within an hour, except 1,4DFB, 3FP. Compared with the result of Rebekka (2012), it was confirmed that the Rh−normalized rate constant of FB was much higher but that of 1,3DFB and 1,4DFB was lower than Rebekka' s results. These results show that even with the same rhodium catalyst, the activity

of the catalyst may vary depending on the type of support.

Table 4.1 Comparison of the pseudo-first-order rate constant of different paper results considering the experimental conditions

Varialbe	Unit	Rh/zeolite			Rh/alumina[1)]		
		FB	1,3DFB	1,4DFB	FB	1,3DFB	1,4DFB
k_{obs}	min^{-1}	0.6026	0.0226	0.0136	0.0617	0.0317	0.0367
k_{obs-Rh}	$min^{-1}(mg_{Rh}/L)^{-1}$	0.1470	0.0055	0.0033	0.0326	0.0168	0.0194
C_0[3)]	μM	200			100		
C_{Rh}[4)]	mg_{Rh}/L	4.1			1.89		
Volume	mL	100			164		

1) Rebekka (2012)

2) $k_{obs-Rh} = k_{obs} / C_{Rh}$

3) C_0 : Initial concentration of the fluoroarene

4) C_{Rh} : Concentration of rhodium in the solution

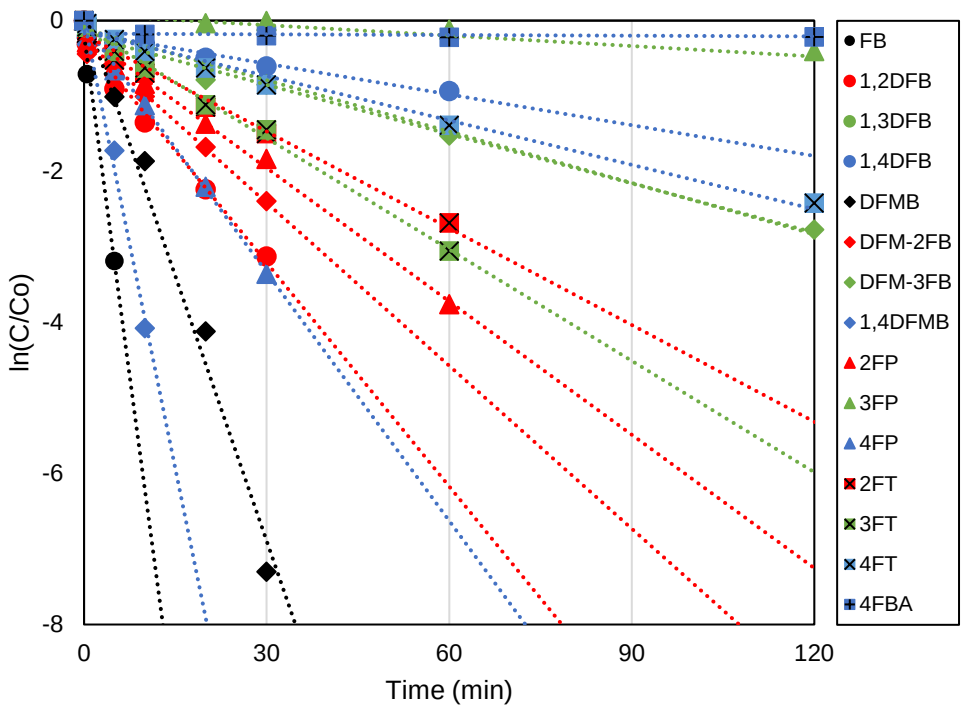

Figure 4.1 Pseudo-first-order kinetic plot of fluoroarene removal by Rh/zeolite catalyst (blank: one substituent, red: ortho, green: meta, blue: para)

4.1.2. Defluorination yield

There is a need to confirm not only how fast the reaction occurs, but also how much defluorination occurs in the overall reaction mechanism. Thus, the fluoride concentration over time during the reaction was measured, and the values were expressed as DeF Yield and DeF ratio as the following definition.

$$\text{DeF yield} = [F^-]_t/[FA]_o$$

$$\text{DeF yield}^* = [F^-]_t/[FA]_o/(\text{No.F})$$

$$\text{DeF ratio}^* = [F^-]_t/([FA]_o-[FA]_t)/(\text{No.F})$$

$[F^-]_t$: Concentration of fluoride at time t [μM]

$[FA]_t$: Concentration of fluoroarene at time t [μM]

$[FA]_o$: Initial concentration of fluoroarene [μM]

No.F : Number of fluorine per molecule

DeF yield is the ratio of the fluoride concentration to the initial concentration of the target material. DeF ratio is the ratio of the concentration of fluoride to the amount of removed target material, meaning that the defluorination mechanism is dominant when the closer the DeF ratio is to 1. The superscript star (*) means normalization by the number of fluorine in the target molecule. All concentration ratio was based on molar concentration.

Defluorination occurred in fluoro and difluoromethyl group, but

much less or no in the trifluoromethyl group. In the case of 4TFMP, it was confirmed that defluorination could occur in the trifluoromethyl group when the hydroxyl group existed in the molecule, but the DeF yield was low to less than 20%. The initial concentration was maintained in the control test when minimizing the headspace volume to prevent it from being volatilized. In other words, the main mechanism of removal of 4TFMP was not defluorination but hydrogenation. Likewise, the main removal mechanism of TFMB and PFEB was expected to be hydrogenation.

Table 4.2 Pseudo-first-order reaction constants and DeF yields of the reaction in the presence of Rh/zeolite catalyst

Fluoroarene	k_{obs}	Log(k_{obs})	DeF yield	DeF yield*
	[min^{-1}]		[mol/mol]	[mol^{-1}]
FB	0.6026	−0.220	0.947	0.947
1,2FB	0.0982	−1.008	1.700	0.850
1,3FB	0.0226	−1.646	1.459	0.729
1,4FB	0.0136	−1.866	1.281	0.641
DFMB	0.2338	−0.631	2.005	1.003
DFM-2FB	0.061	−1.180	2.409	0.803
DFM-3FB	0.0211	−1.676	0.884	0.295
1,4DFMB	0.3962	−0.402	3.442	0.861
2FP	0.0589	−1.230	0.633	0.633
3FP	0.0037	−2.432	0.798	0.798
4FP	0.1087	−0.964	0.950	0.950
2FT	0.0468	−1.330	0.997	0.997
3FT	0.0485	−1.314	0.633	0.633
4FT	0.0196	−1.708	0.995	0.995
4FBA	0.0003	−3.523	0.387	0.387
TFMB	0.0069	−4.976	N.D[1)]	−
4TFMP	0.0085	−4.768	0.341	0.114
PFEB	0.0110	−1.959	1.356	0.271

1) N.D: None detected

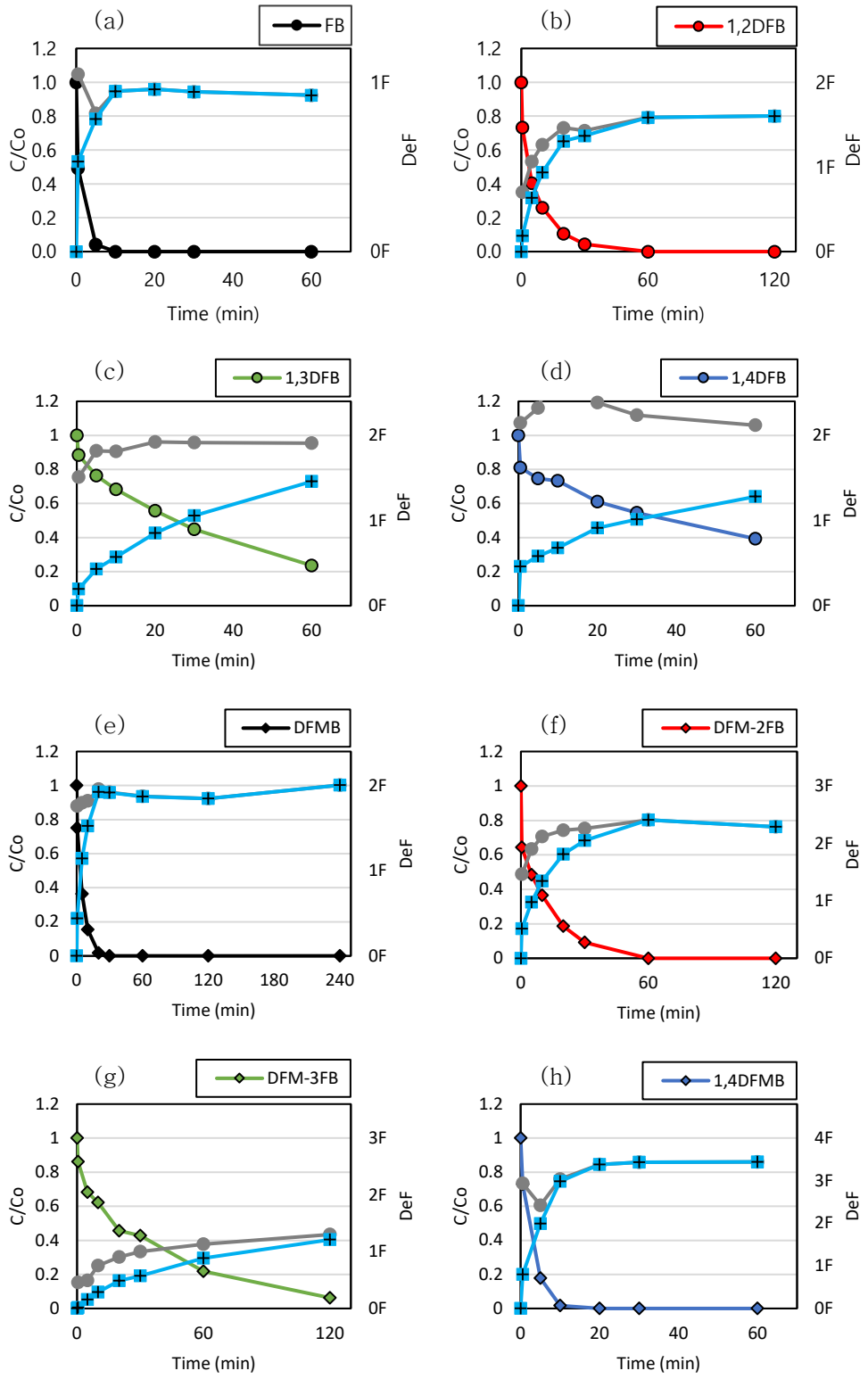
(a)
FB
C/Co
DeF
Time (min)
(b)
1,2DFB
(c)
1,3DFB
(d)
1,4DFB
(e)
DFMB
(f)
DFM-2FB
(g)
DFM-3FB
(h)
1,4DFMB

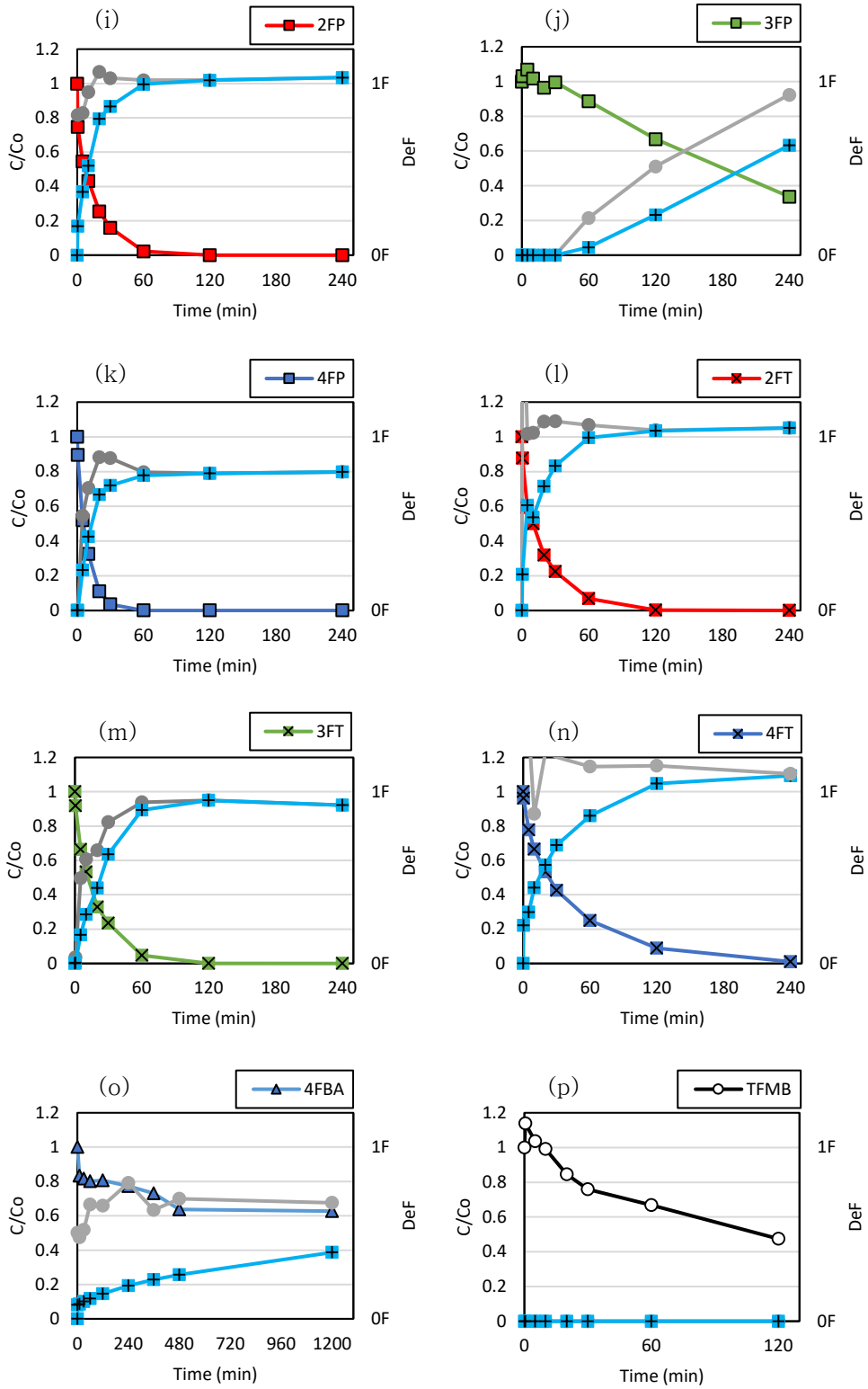
(i)
2FP
(j)
3FP
(k)
4FP
(l)
2FT
(m)
3FT
(n)
4FT
(o)
4FBA
(p)
TFMB
C/Co
DeF
1F
0F
Time (min)

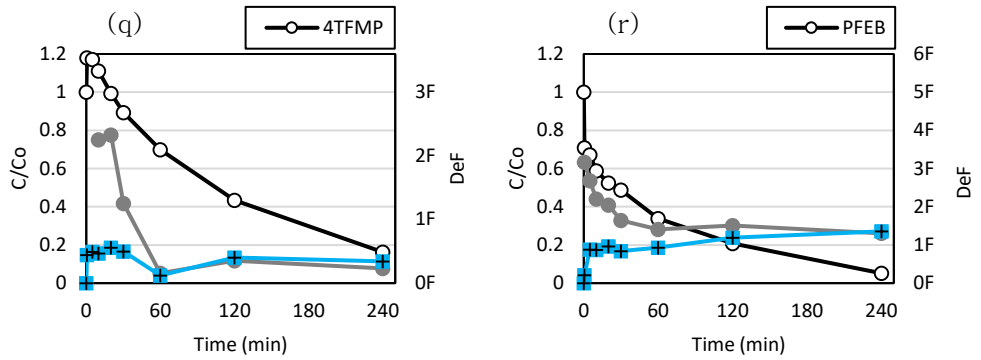

Figure 4.2 Graphs of fluoroarene removal and defluorination yield versus reaction time at pH 7 (phosphate buffer, 10 mM) (✚; DeF yield, ● ; DeF ratio*)

The correlation between Log(k_{obs}) and DeF yield showed weak positive correlations. In other words, rapid removal did not necessarily lead to defluorination. Thus, it was needed to examine the properties of each fluoroarene that affects both Log(k_{obs}) and DeF yield.

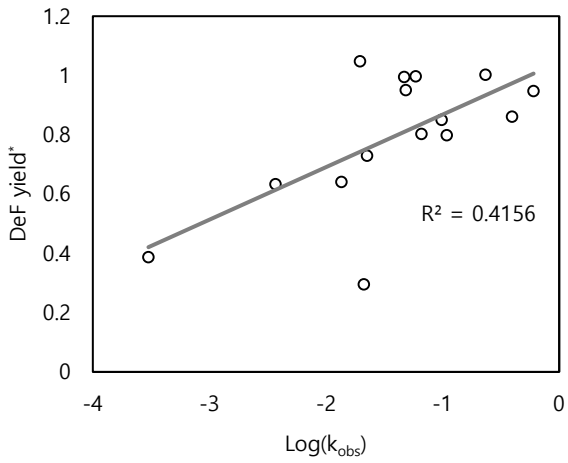

Figure 4.3 Correlation analysis between DeF yield* and Log(k_{obs}) of fluoroarenes

4.2. Effect of structural properties

4.2.1. Effect of the number of fluorine and substituent position

In this study, the reaction rate, and DeF yield* were compared by classifying the number of fluorine (No.F) and the position of the substituent. Fluoroarene with trifluoromethyl or pentafluoroethyl group was excluded from the comparison because the reaction rate was slow compared with other fluoroarenes, the DeF yield was also low or the defluorination reaction did not occur.

In Figure 4.4-(a), No.F did not significantly affect the reaction rate range. On the other hand, in Figure 4.4-(b), it was found that the reaction rate range decreased in the order of one substituent, ortho, and meta position, but the tendency was not continued in the case of para position. Therefore, it was difficult to explain the reactivity of fluoroarene containing difluoromethyl or other functional groups based on only the No.F and position of substituents shown in the existing references. To compensate for this, in the next part, the reactivity was examined according to the type of fluorine substituent and other functional groups.

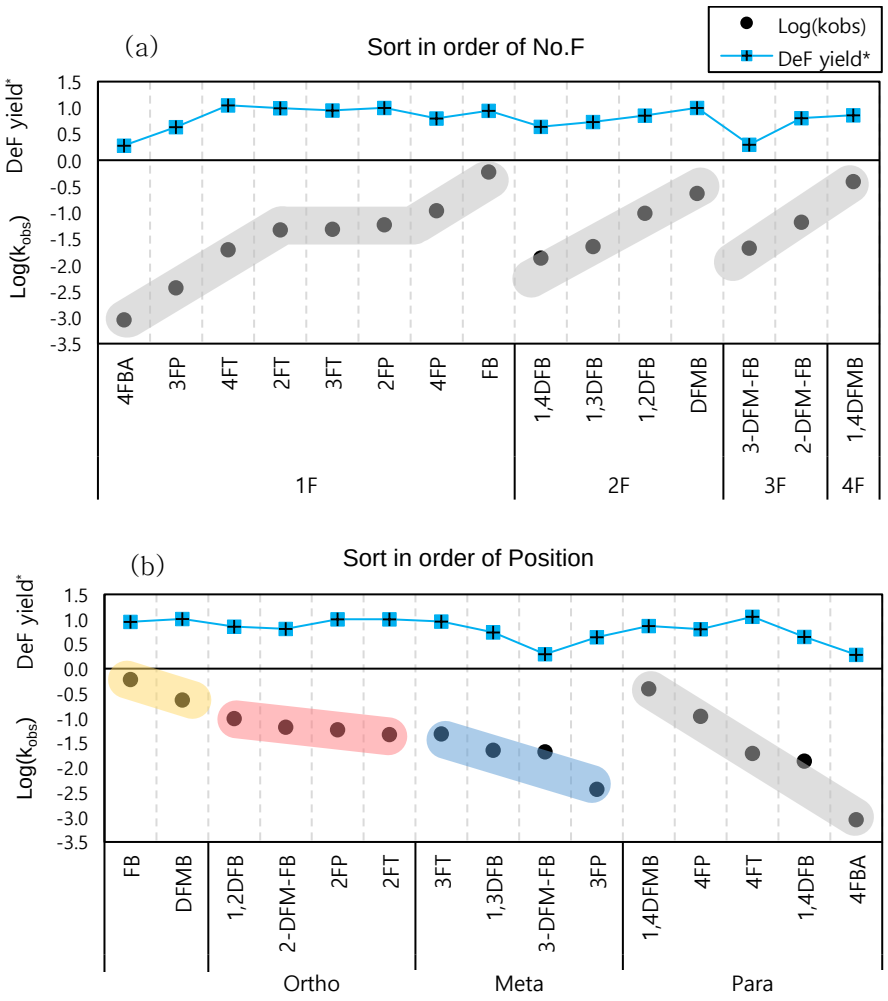

Figure 4.4 Log(k_{obs}) and DeF yield of fluoroarenes in order of (a) number of fluorine (No.F), and (b) position of substituent

4.2.2. Effect of substituent type

There is a difference in DeF yield when comparing fluorine of difluoromethyl substituent group and fluorine directly bound to benzene. In the case of 2DFB and DFM−2FB, the almost maximum amount of fluoride was generated at the target to be removed. In the case of meta−position, the rate constant of DFM−3FB was similar to

3DFB but the final DeF yield* was higher than that of 3DFB, as shown in Figure 4.2 (c) and (g). Different defluorination preferences of the fluorine and difluoromethyl substituents were expected, so DFM-2FB and DFM-3FB were re-experimented to confirm the intermediates. (Difluoromethyl)benzene (DFMB), fluorotoluene (FT), and toluene (T) were selected as the intermediate, and methylcyclohexane (MeCyH) was selected as the final reductant.

As shown in Figure 4.5, the main intermediate of DFM-FB was toluene. DFMB and FT were sharply increased but had a lower proportion compared to the target material and were subsequently removed and also similar in the generated time as well as the C/C_0 ratio. It means that the difference of DeF yield of fluorine bound to benzene and fluorine of difluoromethyl was not due to the substituent type, but the position of the substituent. It was also confirmed that the structural difference had a greater effect on the DeF yield than the reaction rate. The cause was expected because the resonance effect from the π-bond of the arene was higher when it was the ortho than the meta. What was still unknown is the presence of undetected intermediates that did not undergo defluorination but only hydration reaction.

Toluene, the major intermediate in the reduction of DFM-FB, was reduced to MeCyH over time, and MeCyH was expected as a final product in the reduction reaction. However, MeCyH decreased after an hour and the fluoride concentration reached equilibrium, meaning that MeCyH was evaporated from solution to the headspace. The water-based solubility of MeCyH (0.014 g/L at 25℃) is

relatively low than that of toluene (0.52 g/L at 20℃), and it supports the fact that MeCyH had been evaporated. As a result, the reaction pathway of DFM-FB was shown in Figure 4.6.

The reaction rate of fluoroarenes with hydroxyl, methyl, and carboxylic acid group was all lower than that of fluorobenzene, and so did DeF yield*. Fluoroarene with these functional groups did not show a significant difference in the BDE of the C-F bond (Table 4.3) but in the reaction rate and DeF yield* depending on the position of the substituent. Thus, the position of the substituents has a greater effect than the BDE of the C-F bond on the reaction rate or DeF yield, even in the presence of a non-fluorine functional group.

In the presence of the carboxylic acid group, the reaction rate and DeF yield significantly decreased, which appeared to be due to the positive electron affinity of the molecule. High stability of dissolved 4FBA was also expected since 4FBA has a high anion ratio (pKa = 4.14) under experimental conditions of pH 7. Therefore, the Rh/zeolite catalyst seemed to have a limitation in reduction treatment with fluoroarenes that have high positive electron affinity, considering that electron affinity was positive for only 4FBA, while all other comparison fluoroarenes were negative for electron affinity.

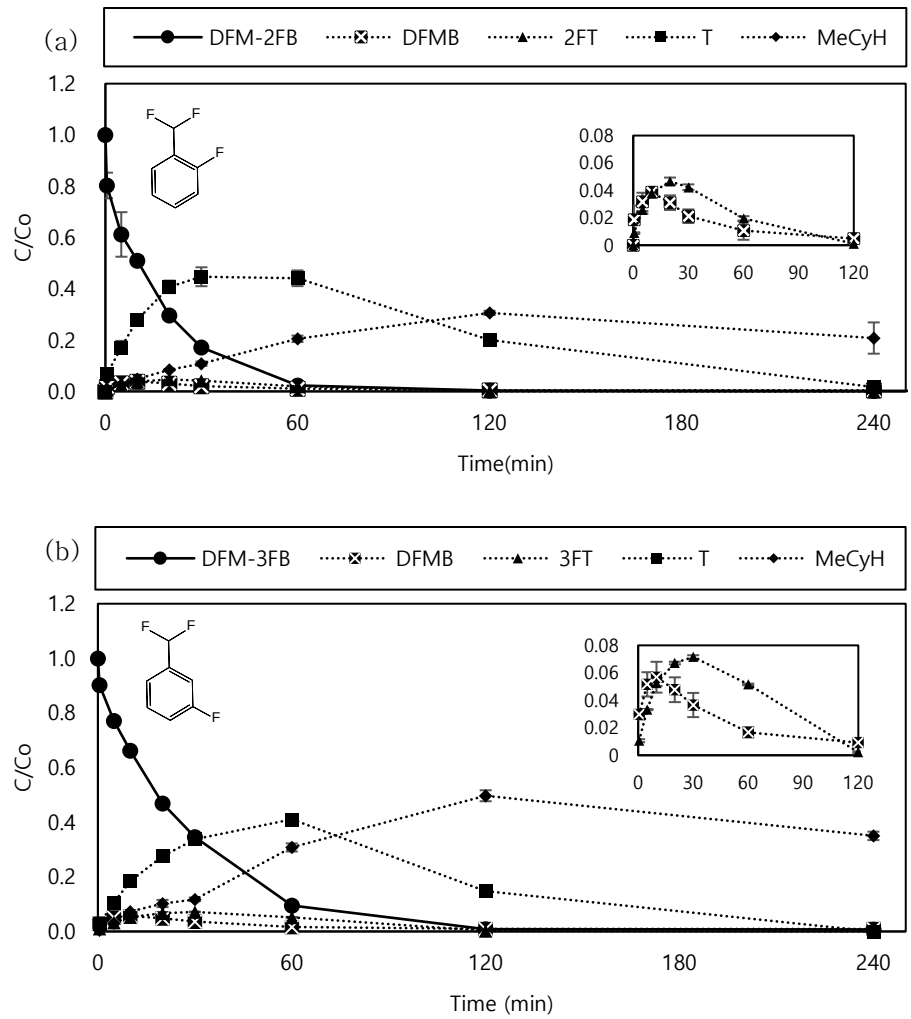

Figure 4.5 Detail of intermediate growth and decay traces during degradation of (a) DFM−2FB and (b) DFM−3FB

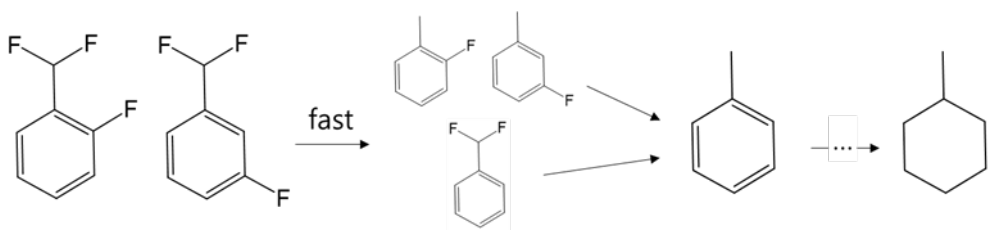

Figure 4.6 Reduction pathway of difluoromethyl−fluorobenzene by Rh/zeolite catalyst

4.3. Structure–reactivity relationships

4.3.1. Selection of variables

According to the previous results, the trend of the reaction rate was not clearly shown depending on the number of fluorine contained in the molecule or the position of the substituents. It means that other variables affected the reactivity of fluoroarenes, thus several chemical properties and new variables suitable for describing fluoroarene were obtained to determine the structure–reactivity relationships using multiple linear regression.

First, the variable representing the position of substituent was needed. Thus, the variable $\sigma_{position}$ was derived, which shows structural properties, based on the fluoro–substituent (FB, 1,2DFB, 1,3DFB, 1,4DFB). The method of deriving the $\sigma_{position}$ is as follows. A linear equation with the slope of −1, and the y–intercept of −0.220 (Log(k_{obs}) of fluorobenzene) was obtained, and then x values were calculated by substituting Log(k_{obs}) of 1,2DFB, 1,3DFB, 1,4DFB for y values. This x values can be understood as the effect of the structural properties on the reaction rate and were defined as $\sigma_{position}$ (one substituent=0.000, ortho=0.788, meta=1.426, para=1.646) (Figure 4.7). The $\sigma_{position}$ was applied to other fluoroarene as shown in Figure 4.8.

Chemical properties of fluoroarenes, such as boiling point (BP), vapor pressure (VP), solubility, electron affinity (EA), and density, were calculated by using SPARC chemical calculator. BP, VP,

solubility, and density were expected to have an indirect effect on catalytic reaction, such as interaction with water molecules or zeolite support. EA was considered to have a correlation with catalytic reaction since it has a high correlation with LUMO energies[23].

The experimental values ($Log(k_{obs})$) as a dependent variable and independent values calculated by SPARC and GAMESS were shown in table 4.3 and Figure A.6.

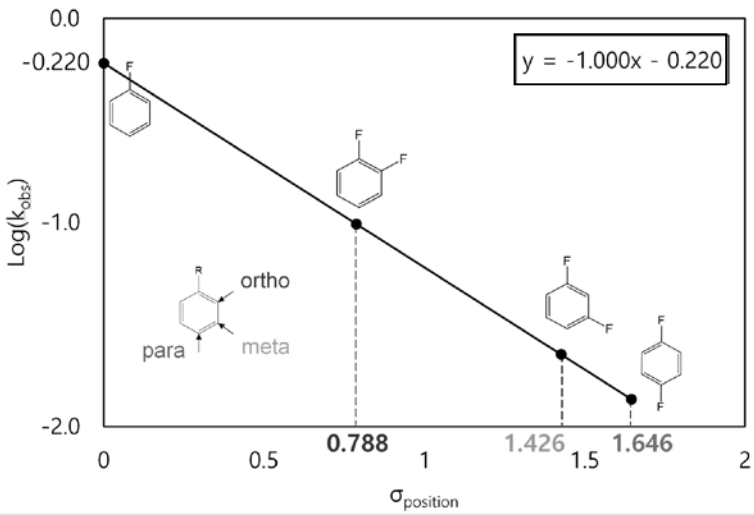

Figure 4.7 The setting of $\sigma_{position}$ variable standardized with fluorobenzenes

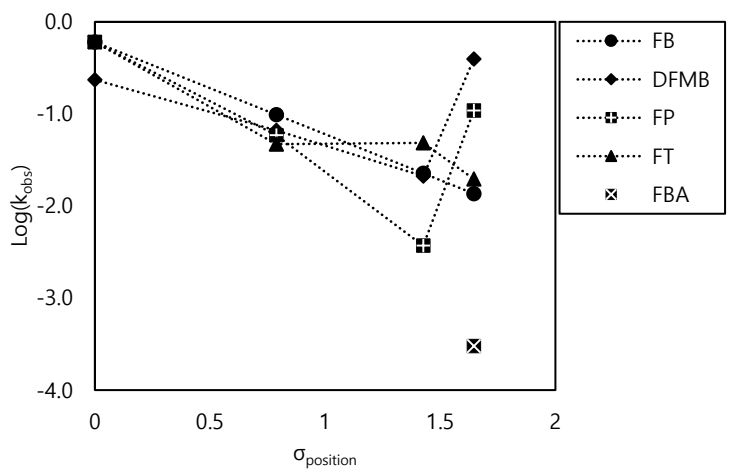

Figure 4.8 $Log(k_{obs})$ values of fluoroarenes versus $\sigma_{position}$ according to substituent type

Table 4.3 Dependent variable ($Log(k_{obs})$) and independent variables used in multiple linear regression analysis

	$Log(k_{obs})$	BP[1)]	VP[1)]	Solubility[1)]	EA[1)]	Density[1)]	BDE[2)]	No.F	$\sigma_{position}$
	[−]	[℃]	[Log(atm)]	[Log(mol/L)]	[eV]	[g/cm^2]	[kJ/mol]	[−]	[−]
FB	−0.220	89.29	−0.99	−1.83	−0.81	1.01	529.357	1	0.000
1,2FB	−1.008	98.07	−1.20	−1.98	−0.46	1.16	520.468	2	0.788
1,3FB	−0.646	82.20	−0.91	−2.00	−0.44	1.15	528.064	2	1.426
1,4FB	−1.866	87.88	−1.01	−1.94	−0.43	1.15	527.540	2	1.646
DFMB	−0.631	116.0	−1.64	−2.18	−0.86	1.09	457.934	2	0.000
DFM−2FB	−1.180	119.5	−1.79	−2.21	−0.30	1.22	462.715	3	0.788
DFM−3FB	−1.676	119.1	−1.76	−2.31	−0.29	1.20	454.574	3	1.426
1,4DFMB	−0.402	137.2	−2.38	−2.68	−0.56	1.22	452.439	4	1.646
2FP	−1.230	150.6	−2.47	0.09	−0.65	1.22	513.616	1	0.788
3FP	−2.432	171.1	−2.92	1 (Miscible)	−0.76	1.23	517.934	1	1.426
4FP	−0.964	170.7	−3.00	0.25	−0.78	1.23	516.065	1	1.646
2FT	−1.330	119.0	−1.59	−2.32	−0.62	1.00	518.783	1	0.788
3FT	−1.314	116.5	−1.53	−2.38	−0.62	0.99	517.641	1	1.426
4FT	−1.708	118.5	−1.57	−2.38	−0.62	0.99	516.726	1	1.646
4FBA	−3.523	233.9	−5.45	−2.18	0.43	1.30	517.695	1	1.646

1) Chemical properties that were calculated by using SPARC chemical calculator (Temperature : 25℃, Pressure : 760 torr)

2) BDE: Bond dissociation energy based on water solution (In case of DFMB and TFMB series, the C−F BDE between benzene ring are written first and fluorine and C−F BDE from fluoromethyl group are written later with star mark*.)

4.3.2. Multiple linear regression analysis

Multiple linear regression analysis for each dependent variables Log(k_{obs}) and DeF yield* was performed using all of the independent variables, as shown in Table A.2 and Table A.3. To discriminate the collinearity between variables, variance increase factors (VIFs) were examined and t-test was conducted for each parameter. If VIF equal or higher than 10, there is multicollinearity between variables[22]. When looking at Table A.2 and A.3, most of VIF values were higher than 10. In the t-test results for each variable, the variable corresponding to the Sig. value of less than 0.05 could be interpreted as a significant variable in multiple regression, however, most of variables with the Sig. value of much higher than 0.05 was in Table A.2 and A.3. Thus, by excluding the variables in order of the highest VIF value and the highest Sig. value, it was possible to obtain the results with all VIF less than 10 and Sig. value less than 0.05 when electron affinity, as shown in Table 4.4 and 4.5. In both cases, R^2 was the highest when the entire variables were included and lower R^2 was obtained when more variables were excluded. Finally, two regression models with 0.795 of R^2 for Log(k_{obs}) and 0.816 of R^2 for DeF yield* were obtained.

The greater the magnitude of t-value, the greater the evidence against the null hypothesis. The criterion is that the independent variables have an effect on the dependent variable when the $|t\text{-value}| \geq 1.96$, and can be regarded as a positive effect when it has positive t-value and a negative effect when it has negative t-value.

In the results of the regression analysis, the magnitude of the t-value of electron affinity was the largest as the negative numbers, indicating that the reaction rate and DeF yield* decreased as the electron affinity increased. The larger the electron affinity, the stronger the molecule tends to acquire electrons[24]. In this reaction, fluorine was brought out with electrons from the molecule for defluorination to occur, thus the reaction of losing electrons in the molecule became difficult.

The $\sigma_{position}$ also had a negative effect on both of the dependent variables, meaning that the reaction rate was lower when the substitution position was more distant. This result was the same as the results of polyfluorobenzene's reduction[8]. On the contrary, No.F had a positive effect on the Log(k_{obs}) and DeF yield* when considering various substituents and it was opposite of the results of FB and DFB. In this study, it was because there were more types of fluoroarenes containing only one fluorine atom and their reaction rate constants and DeF yields were often lower than others were. Therefore, No.F could appear differently with a positive or negative effect depending on the range of the target substance.

BDE had a more significant effect on DeF yield* than reaction rate constant. Thus, it was confirmed that the strength of the C-F bond depending on the chemical structure was an appropriate variable for predicting the efficiency of the defluorination ability of Rh/zeolite catalyst to fluoroarenes, not the reaction kinetics. It was peculiar that the t-value of BDE was positive, which seems to be due to the result that BDE of fluorine from difluoromethyl was calculated lower than

that of fluorine bound to benzene and the DFMB series showed lower overall reaction rate constant and DeF yield than the DFB series.

In the case of the boiling point, although it did not seem to correlate with the DeF yield superficially, it was expected that the reaction was indirectly influenced by the fact that the positive t-value was quite large. For example, a high boiling point means that the intermolecular attraction force is large, so these properties might have influenced the coordination between the target substance and the rhodium particle on the catalyst.

Table 4.4 Results of ANOVA test and coefficients from multiple linear regression analysis with Log(k_{obs}) as a dependent variable

Model Summary			
R	R^2	Std. Error of The Estimate	Durbin−Watson
0.892	**0.795**	0.419429	2.525

ANOVA					
	Sum of squares	df	Mean square	F	Sig.
Regression	7.498	3	2.499	14.207	0.000
Residual	1.935	11	0.176		
Total	9.433	14			

Coefficients				
	Coefficients	t	Sig.	VIF
(Constant)	−2.414	−5.438	0.000	
Electron Affinity	−1.712	−4.390	0.001	1.206
$\sigma_{position}$	−0.468	−2.223	0.048	1.188
No.F	0.376	3.186	0.009	1.025

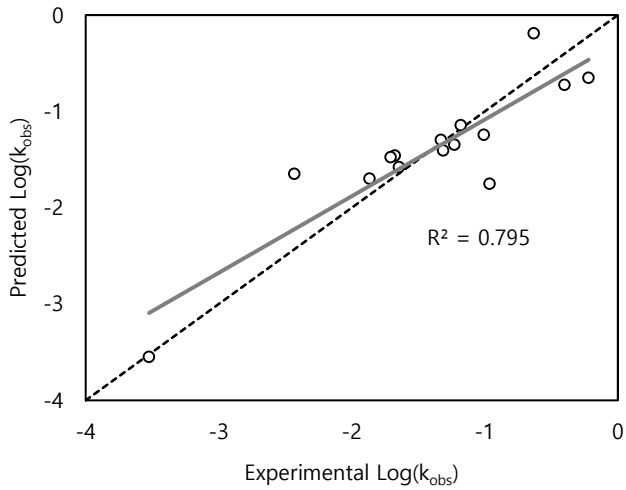

Figure 4.9 Correlation between experimental values and predicted values of Log(k_{obs}) by multiple linear regression

Table 4.5 Correlation between experimental values and predicted values of DeF yield* by multiple linear regression

Model Summary			
R	R^2	Std. Error of The Estimate	Durbin−Watson
0.903	**0.816**	0.121379	1.845

ANOVA					
	Sum of squares	df	Mean square	F	Sig.
Regression	0.586	5	0.117	7.959	0.004
Residual	0.133	9	0.015		
Total	0.719	14			

Coefficients				
	Coefficients	t	Sig.	VIF
(Constant)	−4.825	−2.912	0.017	
Electron Affinity	−0.813	−5.112	0.001	2.394
$\sigma_{position}$	−0.256	−3.470	0.007	1.735
BDE	0.008	3.138	0.012	5.951
Boiling point	0.006	3.795	0.004	3.789
No.F	0.270	2.948	0.016	7.385

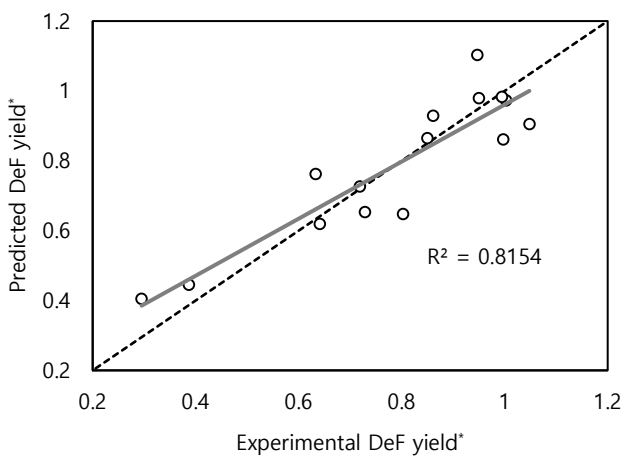

Figure 4.10 Correlation of experimental values and predicted from multiple linear regression analysis with DeF yield* as a dependent variable

5. Conclusions

The Rh/zeolite catalyst synthesized in this study was effective for the defluorination of fluorobenzene but had limitations on perfluoroalkyl groups such as trifluoromethyl and pentafluoroethyl. In the presence of difluoromethyl, the reactivity tended to decrease compared to fluorobenzene, but the reaction rate increased significantly when the molecule had a para position like 1,4DFMB. It was difficult to find a consistent trend for all the fluoroarenes experimented in this study, and it seemed that factors related to several of fluoroarene's characteristics were intertwined.

Two multiple linear regression models were obtained for $Log(k_{obs})$ with R^2 of 0.795 and DeF yield* with R^2 of 0.816. In the regression model for the rate constant, since the dependent variable was log scale, the error corresponding to 1 on the graph was an error of 10 times in the actual reaction rate constant. On the other hand, the regression model for DeF yield* was derived without changing the scale of the dependent variable, so it was judged that a more accurate interpretation of the reaction would be possible than $Log(k_{obs})$. The factors that commonly affected the two dependent variables were (1) electron affinity, (2) $\sigma_{position}$, and (3) No.F. For DeF yield*, a total of five variables were selected by adding (4) BDE and (5) Boiling point. Among them, electron affinity had the greatest effect on both the $Log(k_{obs})$ and DeF yield*, and the reaction rate and defluorination rate were lower when the electron affinity was higher. Similarly, $\sigma_{position}$ had a negative effect, but its influence on $Log(k_{obs})$ was relatively low

compared to DeF yield*. BDE appeared to be a significant variable only in DeF yield*. In other words, the strength of C−F bond was more influential for the final DeF yield rather than the reaction rate. Boiling point as a significant variable in DeF yield* regression was expected to influence indirectly on the reaction, such as the coordination between the target substance and the rhodium particle on the catalyst.

In conclusion, the Log(k_{obs}) and DeF yield* cannot be explained in the same way, and the variables tried in this study were more suitable for predicting DeF yield*. The characteristics of catalyst and the binding force of rhodium−fluoroarene, which were not covered in this study, also could affect on the defluorination reaction of fluoroarene, and the coordination between reactants and metals needs to be further studied.

Appendix

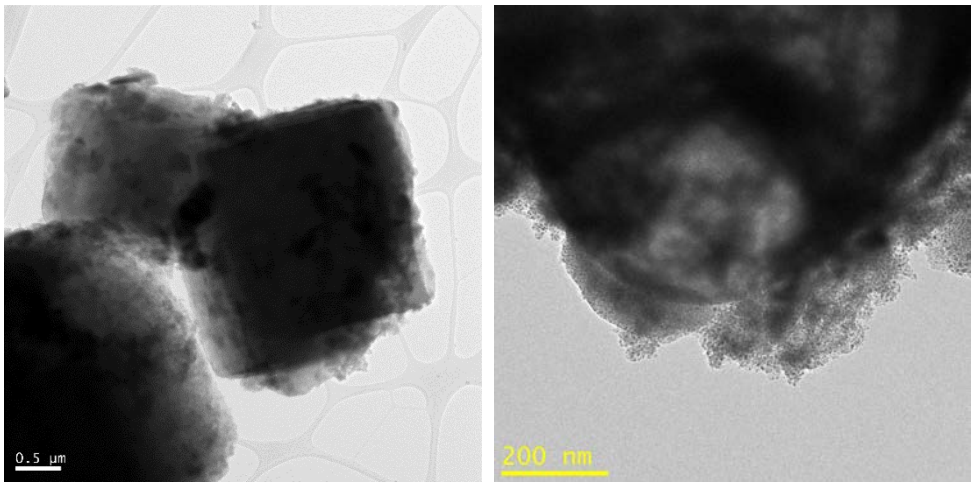

Figure A.1 TEM images of Rh/zeolite catalyst

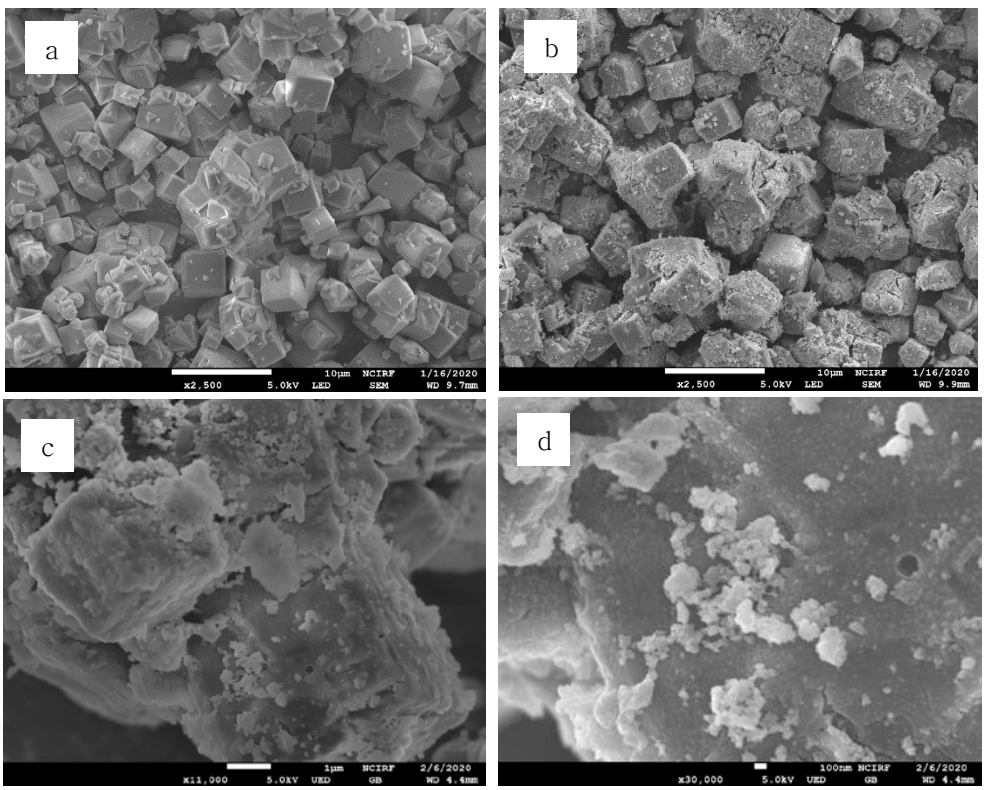

Figure A.2 SEM images of zeolite and Rh/zeolite catalyst (a: zeolite3A, b, c, d: Rh/zeolite)

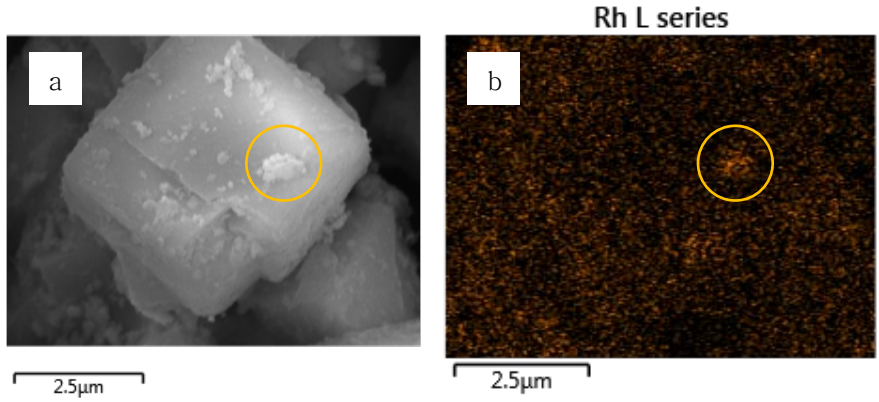

Figure A.3 SEM EDS of Rh/zeolite (a: Electron image, b: atomic mappings)

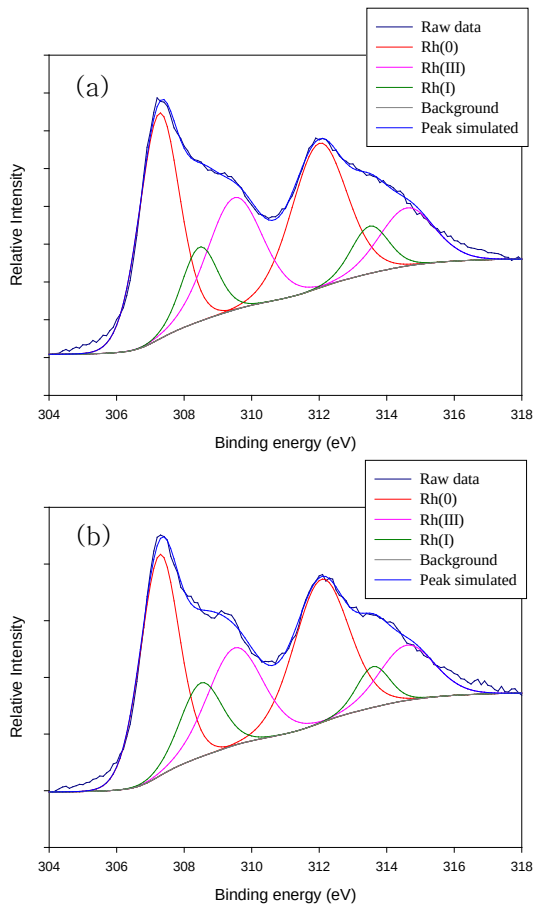

Figure A.4 XPS spectra of (a) Rh/zeolite before reaction and (b) Rh/zeolite catalyst collected after the reaction of penatfluoroethylbeznene[25,26]

Table A.1 SPARC physical and chemical properties calculator statistical performance versus observations[27]

Property	Units	Total# molecule	RMS	R^2	Reaction conditions Temp/Solvent
Vapor pressure	Log atm	747	0.15	0.994	25
Boiling point	℃	4000	5.71	0.994	25
Solubility	Log MF	647	0.40	0.987	25, 41 solvents
Electron affinity	eV	260	0.14	0.98	Gas

Figure A.5 Scatter diagram matrix for all variables

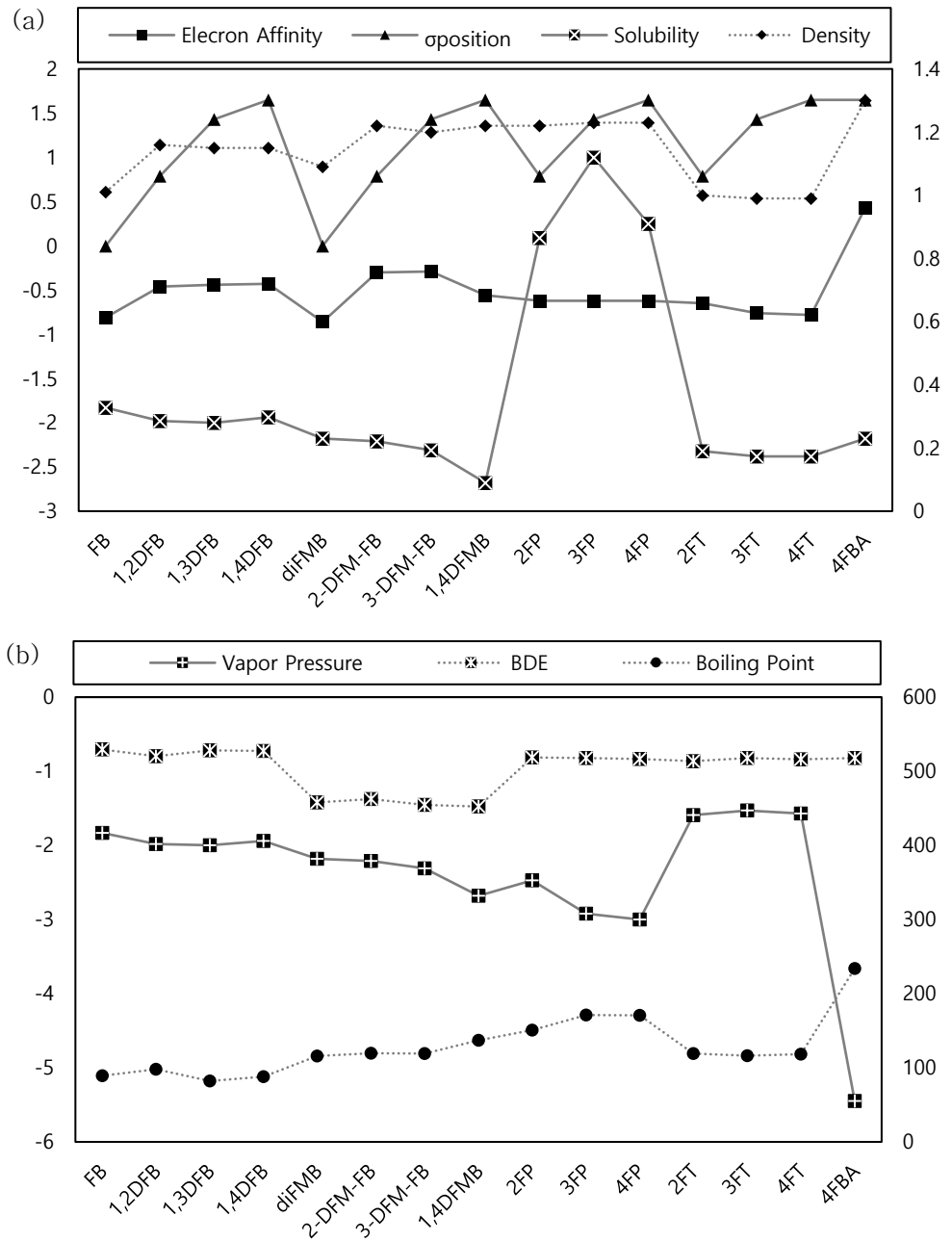

Figure A.6 The calculated values by SPARC and GAMESS (Straight line; left axis, Dotted line; right axis)

Table A.2 Results of ANOVA test and coefficients from multiple linear regression analysis with Log(k_{obs}) as a dependent variable and all chemical properties as independent variables

Model Summary					
R	R^2		Std. Error of The Estimate	Dubin−Watson	
0.924	0.853		0.444766	2.270	
ANOVA					
	Sum of squares	df	Mean square	F	Sig.
Regression	8.106	8	1.013	4.583	0.040
Residual	1.327	6	0.221		
Total	9.433	14			
Coefficients					
	Coefficient	t	Sig.	VIF	
(Constant)	−20.157	−1.743	0.132		
Electron Affinity	−3.309	−2.201	0.070	14.264	
$\sigma_{position}$	−0.670	−1.968	0.097	2.464	
BDE	0.016	1.252	0.257	8.737	
Vapor pressure	0.306	0.513	0.627	21.021	
Boiling point	0.011	0.810	0.440	18.722	
Solubility	−0.537	−1.033	0.341	21.811	
Density	6.570	0.817	0.445	43.537	
No.F	0.427	0.631	0.551	26.840	

Table A.3 Results of ANOVA test and coefficients for multiple linear regression analysis with DeF yield* as a dependent variable and all chemical properties as independent variables

Model Summary					
R	R^2		Std. Error of The Estimate	Durbin−Watson	
0.932	0.869		0.125409	2.016	
ANOVA					
	Sum of squares	df	Mean square	F	Sig.
Regression	0.625	8	0.078	4.964	0.033
Residual	0.094	6	0.016		
Total	0.719	14			
Coefficients					
	Coefficient	t	Sig.	VIF	
(Constant)	−7.397	−2.301	0.061		
Electron Affinity	−0.962	−2.385	0.054	14.439	
$\sigma_{position}$	−0.277	−3.075	0.022	2.423	
BDE	0.009	2.619	0.040	8479	
Vapor pressure	0.197	1.232	0.264	21.289	
Boiling point	0.008	2.208	0.069	18.168	
Solubility	−0.111	−0.800	0.454	22.028	
Density	2.310	1.083	0.321	43.116	
No.F	0.149	0.866	0.420	24.434	

Bibliography

1. Whittlesey, M. K. & Peris, E. Catalytic hydrodefluorination with late transition metal complexes. *ACS Catal.* **4**, 3152–3159 (2014).
2. Key, B. D., Howell, R. D. & Criddle, C. S. Fluorinated organics in the biosphere. *Environ. Sci. Technol.* **31**, 2445–2454 (1997).
3. Sabater, S., Mata, J. A. & Peris, E. Hydrodefluorination of carbon–fluorine bonds by the synergistic action of a ruthenium–palladium catalyst. *Nat. Commun.* **4**, 1–7 (2013).
4. Xu, Y., Ma, H., Ge, T., Chu, Y. & Ma, C. A. Rhodium–catalyzed electrochemical hydrodefluorination: A mild approach for the degradation of fluoroaromatic pollutants. *Electrochem. commun.* **66**, 16–20 (2016).
5. Stanger, K. J. & Angelici, R. J. Hydrodefluorination of fluorobenzene catalyzed by rhodium metal prepared from [Rh(COD)2]+BF4− and supported on SiO2 and Pd−SiO2. *J. Mol. Catal. A Chem.* **207**, 59–68 (2004).
6. Baumgartner, R. & McNeill, K. Hydrodefluorination and hydrogenation of fluorobenzene under mild aqueous conditions. *Environ. Sci. Technol.* **46**, 10199–10205 (2012).
7. Belisle, J. Organic Fluorine in Human Serum: Natural Versus Industrial Sources. *Science (80−.).* **212**, 1509–1510 (1981).
8. Baumgartner, R., Stieger, G. K. & McNeill, K. Complete hydrodehalogenation of polyfluorinated and other polyhalogenated benzenes under mild catalytic conditions. *Environ. Sci. Technol.* **47**, 6545–6553 (2013).
9. Chambers, R. D. *Fluorine in Organic Chemistry*. *Fluorine in Organic Chemistry* (Wiley–Blackwell, 2009). doi:10.1002/9781444305371.

10. Cui, B., Jia, S., Tokunaga, E. & Shibata, N. Defluorosilylation of fluoroarenes and fluoroalkanes. *Nat. Commun.* **9**, 1–8 (2018).
11. Engesser, K.-H., Schmidt, E. & Knackmuss, H.-J. Adaptation of Alcaligenes eutrophus B9 and Pseudomonas sp. B13 to 2-Fluorobenzoate as Growth Substrate. *Appl. Environ. Microbiol.* **39**, 68–73 (1980).
12. Engesser, K.H. & Schulte, P. Degradation of 2-bromo-, 2-chloro- and 2-fluorobenzoate by Pseudomonas putida CLB 250. *FEMS microbioloy Lett.* **60**, 143–147 (1989).
13. Carvalho, M. F., Ferreira, M. I. M., Moreira, I. S., Castro, P. M. L. & Janssen, D. B. Degradation of fluorobenzene by Rhizobiales strain F11 via ortho cleavage of 4-fluorocatechol and catechol. *Appl. Environ. Microbiol.* **72**, 7413–7417 (2006).
14. Holleman, A. F. *Lehrbuch der Anorganischen Chemie*. (Water de Gruyter, 2019).
15. Nova, A., Mas-Ballesté, R. & Lledós, A. Breaking C-F bonds via nucleophilic attack of coordinated ligands: Transformations from C-F to C-X bonds (X= H, N, O, S). *Organometallics* **31**, 1245–1256 (2012).
16. Kuehnel, M. F., Lentz, D. & Braun, T. Synthesis of fluorinated building blocks by transition-metal-mediated hydrodefluorination reactions. *Angew. Chemie - Int. Ed.* **52**, 3328–3348 (2013).
17. Amii, H. & Uneyama, K. C-F bond activation in organic synthesis. *Chem. Rev.* **109**, 2119–2183 (2009).
18. Pike, S. D., Crimmin, M. R. & Chaplin, A. B. Organometallic chemistry using partially fluorinated benzenes. *Chem. Commun.* **53**, 3615–3633 (2017).
19. Schwarzenbach, R. P., Gschwend, P. M. & Imboden, D. M.

Environmental Organic Chemistry. (John Wiley & Sons, 2016).

20. Roberts, A. L., Jeffers, P. M., Wolfe, N. L. & Gschwend, P. M. Structure–Reactivity Relationships in Dehydrohalogenation Reactions of Polychlorinated and Polybrominated Alkanes. *Crit. Rev. Environ. Sci. Technol.* **23**, 1–39 (1993).
21. Blanksby, S. J. & Ellison, G. B. Bond dissociation energies of organic molecules. *Acc. Chem. Res.* **36**, 255–263 (2003).
22. Uyanık, G. K. & Güler, N. A Study on Multiple Linear Regression Analysis. *Procedia – Soc. Behav. Sci.* **106**, 234–240 (2013).
23. Zhan, C. G., Nichols, J. A. & Dixon, D. A. Ionization potential, electron affinity, electronegativity, hardness, and electron excitation energy: Molecular properties from density functional theory orbital energies. *J. Phys. Chem. A* **107**, 4184–4195 (2003).
24. Higashino, S., Saeki, A., Okamoto, K., Tagawa, S. & Kozawa, T. Formation and decay of fluorobenzene radical anions affected by their isomeric structures and the number of fluorine atoms. *J. Phys. Chem. A* **114**, 8069–8074 (2010).
25. Yin, X. *et al.* Behavior, mechanism, and equilibrium studies of rhodium(i) extraction from hydrochloric acid with HMImT. *New J. Chem.* **41**, 10054–10061 (2017).
26. Padeste, C., Cant, N. W. & Trimm, D. L. Reactions of ceria supported rhodium with hydrogen and nitric oxide studied with TPR/TPO and XPS techniques. *Catal. Letters* **28**, 301–311 (1994).
27. Hilal, S. & Karickhoff, S. Verification and validation of the SPARC model. *US Environ.* 44 (2003).

초록

Rh-zeolite 촉매를 이용한 불화 방향족 탄화수소의 환원처리

-화학적 구조가 환원반응상수 및 탈불화에 미치는 영향 규명-

서울대학교 대학원
건설환경공학부
안 선 영

본 연구에서는 화학 산업의 큰 부분을 차지하고 있는 플루오로아렌(fluoroarene) 을 Rh 촉매를 이용하여 환원 처리하는 실험을 수행하였다. 로듐 촉매는 C-H 결합에 대한 C-F 결합을 감소시킬 수 있으며, 따라서 Rh/zeolite 촉매를 합성하여 다양한 구조의 플루오로아렌을 감소시켰다. 실험 대상 물질로 fluorobenzene, difluorobenzene, (difluoromethyl)benzene, (trifluoromethyl)benzene, (pentafluoroethyl)benzene, fluorophenol, fluorotoluene, fluorobenzoic acid 를 선정하여 물질 별 반응속도와 탈불화율을 비교하였다. 반응속도 상수 k_{obs}는 log 를 취하여 변환하고, 탈불화율(defluorination yield; DeF yield) 는 플루오린의 수로 표준화 하여 각 물질들의 반응성과 탈불화 정도를 비교하였다. fluorobenzene과 difluorobenzene 계열 (1,2-difluorobenzene, 1,3-difluorobenzene, 1,4-difluorobenzene) 에서는 작용기가 1개일 때, 2개일 때 ortho, meta, para 순서로 반응속도가 감소하는 결과를 얻었고, 이는 다른 논문들의 결과와 일치하는 결과였다. 그러나 trifluoromethyl, pentafluoroethyl과 같이 perfluoroalkyl에 대해서는 반응이 일어나지 않거나 탈불화율이 30% 이하로 낮게 나타나 과불화 알킬 구조에서는

Rh 촉매 적용에 한계가 있었다.

반응이 일어나지 않거나 탈불화 반응이 잘 일어나지 않았던 물질 ((trifluoromethyl)benzene, 4-trifluoromethylphenol, (pentafluoroethyl)-benzene) 을 제외한 플루오로아렌에 대하여 이들의 구조적 특징이 반응속도 및 탈불화율에 어떤 영향을 미쳤는지 알기 위해 다중회귀분석을 수행하였다. 다중회귀분석을 수행하기 위해서는 2개 이상의 독립변수가 필요했으며, 각 플루오로아렌의 구조적 특징을 대표할 수 있는 변수를 선정하였다. 본 연구에서 독립변수로는 $\sigma_{position}$, Bond dissociation energies (BDE), 불소의 수 (No.F) 그리고 SPARC를 통해 계산한 물질의 화학적 특성값들이 선정되었고, 이 독립변수들을 조합하여 적용하면서 다중회귀분석을 수행하였다. 그 결과 반응속도상수 ($Log(k_{obs})$) 에는 전자친화도 (electron affinity), $\sigma_{position}$, and No.F 가 유의미한 영향이 있었고, 탈불화율 (DeF yield*) 에는 전자친화도, $\sigma_{position}$, BDE, 끓는점 (boiling point), No.F 가 유의미한 영향이 있는 것으로 나타났다. 각각의 회귀모델의 R^2 값은 $Log(k_{obs})$에 대해 0.795, DeF yield*에 대해 0.816 이었으며, 본 연구에서 선정한 변수들로 회귀모델을 적용하였을 때 반응속도보다 탈불화율의 경향을 더 잘 설명할 수 있다는 결론을 얻었다. 즉, 플루오로아렌의 구조적, 화학적 특성은 반응속도보다 최종 탈불화율에 더 큰 영향을 미친다는 것이다. 이는 로듐 촉매에 의해 탈불화반응 뿐만 아니라 수소화반응 (hydrogenation) 또한 함께 일어나고 플루오로아렌의 구조적, 화학적 특성이 탈불화/수소화 반응의 비율을 변화시킬 수 있음을 시사한다.

수소화반응을 통해 생성될 수 있는 중간생성물질의 조합은 매우 많기 때문에 모두 정량할 수는 없었으나, 1-difluoromethyl-2-fluorobenzene 과 1-difluoromethyl-3-fluorobenzene 을 시작물질로 실험하였을 때 예상되는 중간생성물질로

difluoromethylbenzene, fluorotoluene, toluene, methylcyclohexane을 선정하여 반응 시간에 따라 농도를 정량하였다. 그 결과 두 경우 모두 초기 농도 대비 dimethylbenzene과 fluorotoluene의 농도 비율이 매우 낮게 측정되었으며 생성된 시간도 비슷한 수준으로 나타났다. 즉, 벤젠고리에 결합된 불소나 dimethyl의 불소 모두 빠른 속도로 탈불화 반응이 일어날 수 있었으며, 최종 탈불화율의 차이는 불소가 제거되지 않은 채로 수소화반응이 일어난 물질이 생성되었을 가능성이 있다. 이러한 현상은 1,3-difluorobenzene, 1-difluoromethyl-3-fluorobenzene, and 3-fluorophenol 과 같이 두 작용기가 meta 위치에 있을 때 발생하였으며, 3-fluorotoluene에서는 예외였다.

따라서 다양한 구조의 Fluoroarene의 경우 제거 속도와 탈불화율의 경향성은 각각 다른 방식으로 접근하여 처리 효율을 예측할 수 있을 것이며, 기존의 linear chain 구조를 가진 PFCs와는 다른 접근이 필요하다.

주요어: 플루오로아렌, 탈불화반응, 로듐 촉매, 구조-반응 관계식

학번: 2018-26687